

Testing SU(3) Flavor Symmetry in Semileptonic and Two-body Nonleptonic Decays of Hyperons

Ru-Min Wang^{1,†}, Mao-Zhi Yang^{2,*}, Hai-Bo Li^{3,4,§} and Xiao-Dong Cheng^{5,‡}

¹College of Physics and Communication Electronics, JiangXi Normal University, NanChang, JiangXi 330022, China

²School of Physics, Nankai University, TianJin 300071, China

³Institute of High Energy Physics, BeiJing 100049, China

⁴University of Chinese Academy of Sciences, BeiJing 100049, China

⁵College of Physics and Electronic Engineering, XinYang Normal University, XinYang, Henan 464000, China

[†]ruminwang@sina.com

^{*}yangmz@nankai.edu.cn

[§]lihb@ihep.ac.cn

[‡]chengxd@mails.ccnu.edu.cn

The semileptonic decays and two-body nonleptonic decays of light baryon octet (T_8) and decuplet (T_{10}) consisting of light u, d, s quarks are studied with the SU(3) flavor symmetry in this work. We obtain the amplitude relations between different decay modes by the SU(3) irreducible representation approach, and then predict relevant branching ratios by present experimental data within 1σ error. We find that the predictions for all branching ratios except $\mathcal{B}(\Xi \rightarrow \Lambda^0 \pi)$ and $\mathcal{B}(\Xi^* \rightarrow \Xi \pi)$ are in good agreement with present experimental data, that implies the neglected C_+ terms or SU(3) breaking effects might contribute at the order of a few percent in $\Xi \rightarrow \Lambda^0 \pi$ and $\Xi^* \rightarrow \Xi \pi$ weak decays. We predict that $\mathcal{B}(\Xi^- \rightarrow \Sigma^0 \mu^- \bar{\nu}_\mu) = (1.13 \pm 0.08) \times 10^{-6}$, $\mathcal{B}(\Xi^- \rightarrow \Lambda^0 \mu^- \bar{\nu}_\mu) = (1.58 \pm 0.04) \times 10^{-4}$, $\mathcal{B}(\Omega^- \rightarrow \Xi^0 \mu^- \bar{\nu}_\mu) = (3.7 \pm 1.8) \times 10^{-3}$, $\mathcal{B}(\Sigma^- \rightarrow \Sigma^0 e^- \bar{\nu}_e) = (1.35 \pm 0.28) \times 10^{-10}$, $\mathcal{B}(\Xi^- \rightarrow \Xi^0 e^- \bar{\nu}_e) = (4.2 \pm 2.4) \times 10^{-10}$. We also study $T_{10} \rightarrow T_8 P_8$ weak, electromagnetic or strong decays. Some of these decay modes could be observed by the BESIII, LHCb and other experiments in the near future. Due to the very small life times of $\Sigma^0, \Xi^{*0,-}, \Sigma^{*0,-}$ and $\Delta^{0,-}$, the branching ratios of these baryon weak decays are only at the order of $\mathcal{O}(10^{-20} - 10^{-13})$, which are too small to be reached by current experiments. Furthermore, the longitudinal branching ratios of $T_{8A} \rightarrow T_{8B} \ell^- \bar{\nu}_\ell$ ($\ell = \mu, e$) decays are also given.

I. INTRODUCTION

A lot of semileptonic decays and two-body nonleptonic decays of light octet baryons (such as $\Xi^- \rightarrow \Sigma^0 e^- \bar{\nu}_e$, $\Xi^- \rightarrow \Lambda^0 \ell^- \bar{\nu}_\ell$, $\Xi^0 \rightarrow \Sigma^+ \ell^- \bar{\nu}_\ell$, $\Lambda^0 \rightarrow p \ell^- \bar{\nu}_\ell$, $\Sigma^- \rightarrow n \ell^- \bar{\nu}_\ell$, $\Sigma^- \rightarrow \Lambda^0 e^- \bar{\nu}_e$, $\Sigma^+ \rightarrow \Lambda^0 e^+ \nu_e$, $n \rightarrow p e^- \bar{\nu}_e$, $\Sigma^+ \rightarrow p \pi^0$, $\Sigma^+ \rightarrow n \pi^+$, $\Sigma^- \rightarrow n \pi^-$, $\Lambda^0 \rightarrow p \pi^-$, $\Lambda^0 \rightarrow n \pi^0$, $\Xi^- \rightarrow \Lambda^0 \pi^-$, $\Xi^0 \rightarrow \Lambda^0 \pi^0$) and a few light decuplet baryon decays (such as $\Omega^- \rightarrow \Xi^0 e^- \bar{\nu}_e$, $\Xi^0 \pi^-$, $\Xi^- \pi^0$, $\Lambda^0 K^-$) were measured a long time ago by SPEC, HBC, OSPK etc [1]. Now the sensitivity for measurements of $\Lambda, \Sigma, \Xi, \Omega$ hyperon decays is in the range of $10^{-5} - 10^{-8}$ at the BESIII [2–5], and these hyperons are also produced copiously at the LHCb experiment [6, 7]. Besides confirming information obtained earlier by SPEC, HBC, OSPK etc., new information on light baryon decays will be obtained at the BESIII and LHCb experiments. The precise measurements of these decays are of great importance in determining the V-A structure and

quark-flavor mixing of charged current weak interactions [8–10] as well as probing the non-standard charged current interactions [11, 12].

Theoretically, the factorization does not work well for s, d quark decays since s, d quarks are very light and can not use the heavy quark expansion. There is no reliable method to calculate these decay matrix elements at present. In the lack of reliable calculations, the symmetry analysis can provide very useful information about the decays. SU(3) flavor symmetry is one of the symmetries which have attracted a lot of attentions. The SU(3) flavor symmetry approach, which is independent of the detailed dynamics, offers an opportunity to relate different decay modes. Nevertheless, it cannot determine the size of the amplitudes by itself. However, if experimental data are enough, one may use the data to extract the SU(3) irreducible amplitudes, which can be viewed as predictions based on symmetry. There are two popular ways of the SU(3) flavor symmetry. One is to construct the SU(3) irreducible representation amplitude by decomposing effective Hamiltonian. The other way is topological diagram approach, where decay amplitudes are represented by connecting quark line flows in different ways and then relate them by the SU(3) symmetry.

The SU(3) flavor symmetry works well in heavy hadron decays, for instance, the b -hadron decays [13–24] and the c -hadron decays [25–39]. The experimental data of some semileptonic hyperon decays are well explained by the Cabibbo theory [10], which assumes the SU(3) symmetry breaking effects are neglected. The SU(3) flavor symmetry breaking effects are also studied in the hyperon beta-decays [40–43], where it is found that the SU(3) symmetry breaking effects in these decays are small. In this paper, we will systematically study $T_{8,10} \rightarrow T_8 \ell^- \bar{\nu}_\ell$ and $T_{8,10} \rightarrow T_8 P$ decays by the SU(3) irreducible representation approach (IRA). We will firstly construct the SU(3) irreducible representation amplitudes for different kinds of T_8 and T_{10} decays, secondly obtain the decay amplitude relations between different decay modes, then use the available data to extract the SU(3) irreducible amplitudes, and finally predict the not-yet-measured modes for further tests in experiments.

This paper is organized as follows. In Sec. II, the semileptonic weak decays of the $T_{8,10}$ hyperons are studied. In Sec. III, we will explore the two-body nonleptonic decays of hyperons which are through weak interaction, electromagnetic or strong interaction. Our conclusions are given in Sec. IV.

II. Semileptonic decays of hyperons

The light baryons T_8 (T_{10}), which are octet (decuplet) under the SU(3) flavor symmetry of u, d, s quarks, can be written as

$$T_8 = \begin{pmatrix} \frac{\Lambda^0}{\sqrt{6}} + \frac{\Sigma^0}{\sqrt{2}} & \Sigma^+ & p \\ \Sigma^- & \frac{\Lambda^0}{\sqrt{6}} - \frac{\Sigma^0}{\sqrt{2}} & n \\ \Xi^- & \Xi^0 & -\frac{2\Lambda^0}{\sqrt{6}} \end{pmatrix}, \quad (1)$$

$$T_{10} = \frac{1}{\sqrt{3}} \left(\begin{pmatrix} \sqrt{3}\Delta^{++} & \Delta^+ & \Sigma^{*+} \\ \Delta^+ & \Delta^0 & \frac{\Sigma^{*0}}{\sqrt{2}} \\ \Sigma^{*+} & \frac{\Sigma^{*0}}{\sqrt{2}} & \Xi^{*0} \end{pmatrix}, \begin{pmatrix} \Delta^+ & \Delta^0 & \frac{\Sigma^{*0}}{\sqrt{2}} \\ \Delta^0 & \sqrt{3}\Delta^- & \Sigma^{*-} \\ \frac{\Sigma^{*0}}{\sqrt{2}} & \Sigma^{*-} & \Xi^{*-} \end{pmatrix}, \begin{pmatrix} \Sigma^{*+} & \frac{\Sigma^{*0}}{\sqrt{2}} & \Xi^{*0} \\ \frac{\Sigma^{*0}}{\sqrt{2}} & \Sigma^{*-} & \Xi^{*-} \\ \Xi^{*-} & \Xi^{*-} & \sqrt{3}\Omega^- \end{pmatrix} \right). \quad (2)$$

In this section, we focus on $\Delta S = 0$ and $\Delta S = 1$ semileptonic decays of hyperons, which decay through $d \rightarrow u e^- \bar{\nu}_e$ or $s \rightarrow u \ell^- \bar{\nu}_\ell$ transitions, respectively. Since $\Delta S = 2$ semileptonic decays are forbidden, we will not study them in this work.

A. $T_{8A} \rightarrow T_{8B} \ell^- \bar{\nu}_\ell$ semileptonic decays

In the Standard Model (SM), the feynman diagram for $T_{8A} \rightarrow T_{8B} \ell^- \bar{\nu}_\ell$ decays is shown in Fig. 1, and the amplitudes of $T_{8A} \rightarrow T_{8B} \ell^- \bar{\nu}_\ell$ can be written as [44]

$$\mathcal{A}(T_{8A} \rightarrow T_{8B} \ell^- \bar{\nu}_\ell) = \sum_{\lambda_W, \lambda'_W = \pm 1, 0, t} \frac{G_F}{2\sqrt{2}} H_{\lambda_B \lambda_W} \bar{u}_\ell \gamma_\beta (1 - \gamma_5) v_\nu \epsilon^{*\beta}(\lambda'_W) g_{\lambda_W \lambda'_W}, \quad (3)$$

with

$$\begin{aligned} H_{\lambda_B \lambda_W} &= H_{\lambda_B \lambda_W}^V - H_{\lambda_B \lambda_W}^A, \quad H_{\lambda_B \lambda_W}^{V(A)} = \langle T_{8B} | J_\mu^{V(A)} | T_{8A} \rangle \epsilon^\mu(\lambda_W), \\ H_{\frac{1}{2}0}^V &= \frac{\sqrt{Q_-}}{\sqrt{q^2}} \left[(m_A + m_B) f_1(q^2) - q^2 f_2(q^2) \right], \\ H_{\frac{1}{2}0}^A &= \frac{\sqrt{Q_+}}{\sqrt{q^2}} \left[(m_A - m_B) g_1(q^2) + q^2 g_2(q^2) \right], \\ H_{\frac{1}{2}1}^V &= \sqrt{2Q_-} \left[-f_1(q^2) + (m_A + m_B) f_2(q^2) \right], \\ H_{\frac{1}{2}1}^A &= \sqrt{2Q_+} \left[-g_1(q^2) - (m_A - m_B) g_2(q^2) \right], \\ H_{\frac{1}{2}t}^V &= \frac{\sqrt{Q_+}}{\sqrt{q^2}} \left[(m_A - m_B) f_1(q^2) + q^2 f_3(q^2) \right], \\ H_{\frac{1}{2}t}^A &= \frac{\sqrt{Q_-}}{\sqrt{q^2}} \left[(m_A + m_B) g_1(q^2) - q^2 g_3(q^2) \right], \end{aligned} \quad (4)$$

where $q = p_A - p_B$ and $Q_\pm = (m_A \pm m_B)^2 - q^2$. Either from parity or from explicit calculation, we have the relations $H_{-\lambda_2 - \lambda_1}^V = H_{\lambda_2 \lambda_1}^V$, $H_{-\lambda_2 - \lambda_1}^A = -H_{\lambda_2 \lambda_1}^A$. The form factors $f_i(q^2)$ and $g_i(q^2)$ are defined by [24]

$$\begin{aligned} \langle T_{8B}(p_B, \lambda_B) | \bar{c} \gamma_\mu b | T_{8A}(p_A, \lambda_A) \rangle &= \bar{u}_B(p_B, \lambda_B) [f_1(q^2) \gamma_\mu + i f_2(q^2) \sigma_{\mu\nu} q^\nu + f_3(q^2) q_\mu] u_A(p_A, \lambda_A), \\ \langle T_{8B}(p_B, \lambda_B) | \bar{c} \gamma_\mu \gamma^5 b | T_{8A}(p_A, \lambda_A) \rangle &= \bar{u}_B(p_B, \lambda_B) [g_1(q^2) \gamma_\mu + i g_2(q^2) \sigma_{\mu\nu} q^\nu + g_3(q^2) q_\mu] \gamma^5 u_A(p_A, \lambda_A). \end{aligned} \quad (5)$$

In term of the SU(3) IRA, the helicity amplitudes $H_{\lambda_B \lambda_W}^{V(A)}$ can be parameterized as

$$H_{\lambda_B \lambda_W}^{V(A)} = a_{n1} H_n^k(T_8)^{[ij]n}(T_8)_{[ij]k} + a_{n2} H_n^k(T_8)^{[ij]n}(T_8)_{[ik]j} + a_{n3} H_n^k(T_8)^{[in]j}(T_8)_{[ij]k}$$

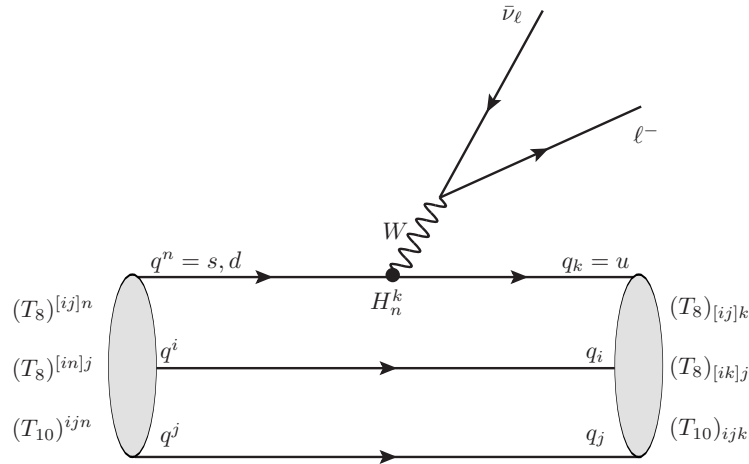


FIG. 1: Feynman diagram for semileptonic weak decays $T_{8,10} \rightarrow T_8 \ell^- \bar{\nu}_\ell$.

$$+a_{n4}H_n^k(T_8)^{[in]j}(T_8)_{[ik]j} + a_{n5}H_n^k(T_8)^{[in]j}(T_8)_{[kj]i}, \quad (6)$$

where $H_n^k = V_{q_k q_n}$ is the CKM matrix element, $a_{ni} \equiv (a_{ni})_{\lambda_B \lambda_W}^{V(A)}(q^2)$ are the nonperturbative coefficients, and $n = 2(3)$ for $q^n = d(s)$. The SU(3) IRA helicity amplitudes $H_{\lambda_B \lambda_W}^{V(A)}$ are listed in the second column of Table I. The helicity amplitudes can be simplified by the redefinitions

$$\begin{aligned} A_{n1} &= a_{n1} + a_{n2} + a_{n3} + a_{n5}, \\ A_{n2} &= a_{n4} - a_{n5}. \end{aligned} \quad (7)$$

For convenience, we set $\bar{A}_{22} = A_{21} - A_{22}$ to replace A_{22} for $d \rightarrow u\ell^- \bar{\nu}_\ell$ transition. The reparameterization results are given in the last column of Table I, in which we can easily see the helicity amplitude relations between different decay modes.

The differential branching ratios of $T_{8A} \rightarrow T_{8B}\ell^- \bar{\nu}_\ell$ decays can be written as

$$\frac{d\mathcal{B}(T_{8A} \rightarrow T_{8B}\ell^- \bar{\nu}_\ell)}{dq^2} = \frac{G_F^2 |V_{uq_n}|^2 \tau_A |\vec{p}_B|^2 q^2}{192\pi^3 m_A^2} \left(1 - \frac{m_\ell^2}{q^2}\right)^2 \left[B_1 + \frac{m_\ell^2}{2q^2} B_2\right], \quad (8)$$

with

$$\begin{aligned} B_1 &= \left|H_{\frac{1}{2}0}\right|^2 + \left|H_{-\frac{1}{2}0}\right|^2 + \left|H_{\frac{1}{2}1}^2\right|^2 + \left|H_{-\frac{1}{2}1}\right|^2, \\ B_2 &= \left|H_{\frac{1}{2}0}\right|^2 + \left|H_{-\frac{1}{2}0}\right|^2 + \left|H_{\frac{1}{2}1}\right|^2 + \left|H_{-\frac{1}{2}1}\right|^2 + 3\left(\left|H_{\frac{1}{2}t}\right|^2 + \left|H_{-\frac{1}{2}t}\right|^2\right). \end{aligned} \quad (9)$$

TABLE I: The helicity amplitudes $H_{\lambda_B \lambda_W}^{V(A)}$ of $T_{8A} \rightarrow T_{8B}\ell^- \bar{\nu}_\ell$ decays.

$H_{\lambda_B \lambda_W}^{V(A)}$	SU(3) IRA amplitudes	Reparameterization
$s \rightarrow u\ell^- \bar{\nu}_\ell :$		
$\sqrt{2}H(\Xi^- \rightarrow \Sigma^0 \ell^- \bar{\nu}_\ell)$	$-(a'_{31} + a'_{32} + a'_{33} + a'_{35})$	$-A_{31}$
$\sqrt{6}H(\Xi^- \rightarrow \Lambda^0 \ell^- \bar{\nu}_\ell)$	$a'_{31} + a'_{32} + a'_{33} + 2a'_{34} - a'_{35}$	$A_{31} + 2A_{32}$
$H(\Xi^0 \rightarrow \Sigma^+ \ell^- \bar{\nu}_\ell)$	$a'_{31} + a'_{32} + a'_{33} + a'_{35}$	A_{31}
$\sqrt{6}H(\Lambda^0 \rightarrow p\ell^- \bar{\nu}_\ell)$	$-(2a'_{31} + 2a'_{32} + 2a'_{33} + a'_{34} + a'_{35})$	$-(2A_{31} + A_{32})$
$\sqrt{2}H(\Sigma^0 \rightarrow p\ell^- \bar{\nu}_\ell)$	$a'_{34} - a'_{35}$	A_{32}
$H(\Sigma^- \rightarrow n\ell^- \bar{\nu}_\ell)$	$-(a'_{34} - a'_{35})$	$-A_{32}$
$d \rightarrow ue^- \bar{\nu}_e :$		
$\sqrt{2}H(\Sigma^- \rightarrow \Sigma^0 e^- \bar{\nu}_e)$	$-(a'_{21} + a'_{22} + a'_{23} + a'_{24})$	$-(2A_{21} - \bar{A}_{22})$
$\sqrt{6}H(\Sigma^- \rightarrow \Lambda^0 e^- \bar{\nu}_e)$	$a'_{21} + a'_{22} + a'_{23} - a'_{24} + 2a'_{22}$	\bar{A}_{22}
$\sqrt{2}H(\Sigma^0 \rightarrow \Sigma^+ e^- \bar{\nu}_e)$	$a'_{21} + a'_{22} + a'_{23} + a'_{24}$	$2A_{21} - \bar{A}_{22}$
$\sqrt{6}H(\Sigma^+ \rightarrow \Lambda^0 e^+ \nu_e)$	$a'_{21} + a'_{22} + a'_{23} - a'_{24} + 2a'_{22}$	\bar{A}_{22}
$H(\Xi^- \rightarrow \Xi^0 e^- \bar{\nu}_e)$	$-a_{22}$	$\bar{A}_{22} - A_{21}$
$H(n \rightarrow pe^- \bar{\nu}_e)$	$a'_{21} + a'_{22} + a'_{23} + a'_{22}$	A_{21}

The differential longitudinal branching ratios $d\mathcal{B}^L(T_{8A} \rightarrow T_{8B}\ell^-\bar{\nu}_\ell)/dq^2$ can be obtained from $d\mathcal{B}(T_{8A} \rightarrow T_{8B}\ell^-\bar{\nu}_\ell)/dq^2$ by setting $|H_{\frac{1}{2}1}^2|^2 = |H_{-\frac{1}{2}-1}|^2 = 0$ in Eqs. (8-9).

The theoretical input parameters and the experimental data within the 1σ error from Particle Data Group [1] will be used in our numerical results. Two cases will be considered in our analysis:

S_1 : Neglecting B_2 term in Eq. (8) as in Ref. [35] and treating $SU(3)$ flavor parameters $(a_{ni})_{\lambda_B\lambda_W}^{V(A)}(q^2)$ as constants without the q^2 dependence, *i.e.* B_1 in Eq. (8) is constant. Then there are three parameters

$$\begin{aligned} A_{31}, A_{32}e^{i\delta_{A_{32}}} & \quad \text{for } s \rightarrow u\ell^-\bar{\nu}_\ell \text{ transition,} \\ A_{21}, \bar{A}_{22}e^{i\delta_{\bar{A}_{22}}} & \quad \text{for } d \rightarrow u\ell^-\bar{\nu}_e \text{ transition.} \end{aligned} \quad (10)$$

Noted that, A_{31} , A_{32} , A_{21} and \bar{A}_{22} could be complex. In this work, we set $A_{31}(A_{21})$ is real and add relative phase $\delta_{A_{32}}(\delta_{\bar{A}_{22}})$ associated with $A_{32}(\bar{A}_{22})$.

For $s \rightarrow u\mu^-\bar{\nu}_\mu$ and $s \rightarrow u\ell^-\bar{\nu}_\ell$ transitions, firstly, we use the experimental measurements of $\mathcal{B}(\Xi^0 \rightarrow \Sigma^+e^-\bar{\nu}_e)$ and $\mathcal{B}(\Sigma^- \rightarrow ne^-\bar{\nu}_e)$ to obtain $|A_{31}|$ and $|A_{32}|$, secondly, we use the data of $\mathcal{B}(\Lambda^0 \rightarrow pe^-\bar{\nu}_e)$ to constrain $\delta_{A_{32}}$, which varies in the region $[-180^\circ, 180^\circ]$, and then we give the predictions of relevant branching ratios. For $d \rightarrow u\ell^-\bar{\nu}_e$ transition, we use the experimental measurements of $\mathcal{B}(n \rightarrow pe^-\bar{\nu}_e)$ and $\mathcal{B}(\Sigma^- \rightarrow \Lambda^0e^-\bar{\nu}_e)$ to obtain $|A_{21}|$ and $|\bar{A}_{22}|$, and then let the predictions satisfy other two experimental measurements.

S_2 : In order to obtain more precise predictions, we use the helicity amplitudes in Eq. (4). The form factors for the hyperon semileptonic decays are calculated in various approaches, for examples, quark and soliton models, $1/N_c$ expansion of QCD, lattice QCD and chiral perturbation theory etc [42, 45–54]. In this case, we choose the dipole behavior for the form factors as [40, 51]

$$F_i(q^2) = \frac{F_i(0)}{(1 - q^2/M^2)^2}, \quad (11)$$

where $M = 0.97$ (1.25) GeV for the vector (axial vector) form factors f_i (g_i) in $s \rightarrow u\ell^-\bar{\nu}_\ell$ decays, and $M = 0.84 \pm 0.04$ (1.08 ± 0.08) GeV for f_i (g_i) in $d \rightarrow u\ell^-\bar{\nu}_e$ decays. For the form factor ratios $g_1(0)/f_1(0)$ and $f_2(0)/f_1(0)$, they are preferentially taken from experimental measurements. If no relevant experimental measurements are available, they will be taken from Cabibbo theory [51]. The form factor ratios in Tab. II will be used in our results. As a result, the branching ratios only depend on the form factor $f_1(0)$ and the CKM matrix element V_{uq_n} . Then these three parameters become

$$\begin{aligned} A'_{31}, A'_{32}e^{i\delta_{A'_{32}}} & \quad \text{for } s \rightarrow u\ell^-\bar{\nu}_\ell \text{ transition,} \\ A'_{21}, \bar{A}'_{22}e^{i\delta_{\bar{A}'_{22}}} & \quad \text{for } d \rightarrow u\ell^-\bar{\nu}_e \text{ transition,} \end{aligned} \quad (12)$$

where A'_{ni} contains $f_1(0)$ but without the q^2 dependence. Finally, all experimental data will be considered to constrain these parameters and predict the not-yet-measured branching ratios.

Firstly, we give a comment on the results of the twelve $s \rightarrow u\ell^-\bar{\nu}_\ell$ decay modes. In S_1 case, we get $A_{31} = 5.87 \pm 0.21$, $A_{32} = 2.57 \pm 0.06$, $|\delta_{A_{32}}| \leq 155.90^\circ$ and the predictions are listed in the second column of Tab. III. One can see that when the branching ratio predictions satisfy the data of $\mathcal{B}(\Xi^0 \rightarrow \Sigma^+e^-\bar{\nu}_e)$, $\mathcal{B}(\Sigma^- \rightarrow ne^-\bar{\nu}_e)$ and $\mathcal{B}(\Lambda^0 \rightarrow pe^-\bar{\nu}_e)$, the predictions of $\mathcal{B}(\Xi^- \rightarrow \Lambda^0e^-\bar{\nu}_e)$ and $\mathcal{B}(\Xi^- \rightarrow \Lambda^0\mu^-\bar{\nu}_\mu)$ obviously deviate from their experimental data. In S_2 case,

TABLE II: The form factor ratios $g_1(0)/f_1(0)$ and $f_2(0)/f_1(0)$ from PDG2018 [1] unless otherwise specified. ^adenotes that the values are obtained from the SU(3)-favour parametrization F and D given in Refs. [40, 51] and the measured form factor ratios in Ref. [1], and ^bdenotes that the values are taken from Cabibbo theory [51].

Decay modes	$g_1(0)/f_1(0)$	$f_2(0)/f_1(0)$
$\Xi^- \rightarrow \Sigma^0 \ell^- \bar{\nu}_\ell$	1.22 ± 0.05^a	2.609^b
$\Xi^- \rightarrow \Lambda^0 \ell^- \bar{\nu}_\ell$	0.25 ± 0.05	0.085^b
$\Xi^0 \rightarrow \Sigma^+ \ell^- \bar{\nu}_\ell$	1.22 ± 0.05	2.0 ± 0.9
$\Lambda^0 \rightarrow p \ell^- \bar{\nu}_\ell$	0.718 ± 0.015	1.066^b
$\Sigma^0 \rightarrow p \ell^- \bar{\nu}_\ell$	-0.340 ± 0.017^a	-1.292^b
$\Sigma^- \rightarrow n \ell^- \bar{\nu}_\ell$	-0.340 ± 0.017	-0.97 ± 0.14
$\Sigma^- \rightarrow \Sigma^0 e^- \bar{\nu}_e$	$\frac{1}{2}[(1.2724 \pm 0.0023) + (-0.340 \pm 0.017)]^a$	0.534^b
$\Sigma^- \rightarrow \Lambda^0 e^- \bar{\nu}_e$	$(-0.01 \pm 0.10)^{-1}$	1.490^b
$\Sigma^0 \rightarrow \Sigma^+ e^- \bar{\nu}_e$	$-\frac{1}{2}[(1.2724 \pm 0.0023) + (-0.340 \pm 0.017)]^a$	0.531^b
$\Sigma^+ \rightarrow \Lambda^0 e^+ \nu_e$	$(-0.01 \pm 0.10)^{-1a}$	1.490^b
$\Xi^- \rightarrow \Xi^0 e^- \bar{\nu}_e$	-0.340 ± 0.017^a	-1.432^b
$n \rightarrow p e^- \bar{\nu}_e$	1.2724 ± 0.0023	1.855^b

we consider q^2 -dependence of the form factors and all relevant experimental constraints. We get $A'_{31} = 1.04 \pm 0.04$, $A'_{32} = 0.98 \pm 0.03$, $|\delta_{A'_{32}}| \leq 28^\circ$, and the branching ratio predictions are given in the third column of Tab. III. We can see that the experimental data of $\mathcal{B}(\Xi^- \rightarrow \Lambda^0 e^- \bar{\nu}_e, \Xi^0 \rightarrow \Sigma^+ e^- \bar{\nu}_e, \Lambda^0 \rightarrow p e^- \bar{\nu}_e, \Sigma^- \rightarrow n e^- \bar{\nu}_e, \Sigma^- \rightarrow n \mu^- \bar{\nu}_\mu)$ give the finally effective constraints on the relevant parameters, and the SU(3) IRA predictions in S_2 case are quite consistent with the present data within 1σ error. We predict that $\mathcal{B}(\Xi^- \rightarrow \Sigma^0 \mu^- \bar{\nu}_\mu)$ is at 10^{-6} order of magnitude, which is promising to be observed by the BESIII and LHCb experiments.

Then we comment the results of the six $d \rightarrow u e^- \bar{\nu}_e$ decay modes. Three branching ratios $\mathcal{B}(\Sigma^- \rightarrow \Lambda^0 e^- \bar{\nu}_e)$, $\mathcal{B}(\Sigma^+ \rightarrow \Lambda^0 e^+ \nu_e)$ and $\mathcal{B}(n \rightarrow p e^- \bar{\nu}_e)$ are precisely measured, which can be used to constrain on $A_{21}^{(\prime)}$ and $\bar{A}_{22}^{(\prime)}$ but not on the relative phase $\delta_{\bar{A}_{22}^{(\prime)}}$, so we have quite large errors in the predictions of $\mathcal{B}(\Sigma^- \rightarrow \Sigma^0 e^- \bar{\nu}_e, \Sigma^0 \rightarrow \Sigma^+ e^- \bar{\nu}_e, \Xi^- \rightarrow \Xi^0 e^- \bar{\nu}_e)$. We obtain $A_{21} = 4.61 \pm 0.01$ and $\bar{A}_{22} = 5.85 \pm 0.16$ in S_1 case as well as $A'_{21} = 4.50 \pm 0.02$ and $\bar{A}'_{22} = 0.36 \pm 0.36$ in S_2 case. The predictions for $\mathcal{B}(\Sigma^- \rightarrow \Sigma^0 e^- \bar{\nu}_e, \Sigma^0 \rightarrow \Sigma^+ e^- \bar{\nu}_e, \Xi^- \rightarrow \Xi^0 e^- \bar{\nu}_e)$ in S_2 case are obviously different from that in S_1 case. We predict that $\mathcal{B}(\Sigma^- \rightarrow \Sigma^0 e^- \bar{\nu}_e, \Xi^- \rightarrow \Xi^0 e^- \bar{\nu}_e)$ are at the order of 10^{-10} in S_2 case, which should be tested by the future experiments.

The longitudinal branching ratios of $T_{8A} \rightarrow T_{8B} \ell^- \bar{\nu}_\ell$ decays are also predicted in S_2 case, which are listed in the last column of Tab. III. Noted that the life time of Σ^0 is very small, so the relevant decay branching ratios are also very small, and the same things happen in latter $\Xi^{*0,-}$, $\Sigma^{*0,-}$ and $\Delta^{0,-}$ semileptonic decays.

TABLE III: The experimental data and the SM predictions with the $\pm 1\sigma$ error bar of branching ratios of $T_{8A} \rightarrow T_{8B}\ell\nu_\ell$. ‡ denotes which experimental data give the finally effective constraints on the parameters, and † denotes the predictions depend on the relative phase, which is not constrained well from present data.

Observables	Exp. Data [1]	$\mathcal{B}r - S_1$	$\mathcal{B}r - S_2$	$\mathcal{B}r^L - S_2$
$\mathcal{B}(\Xi^- \rightarrow \Sigma^0 e^- \bar{\nu}_e)(\times 10^{-5})$	8.7 ± 1.7	8.12 ± 0.60	8.27 ± 0.58	5.23 ± 0.35
$\mathcal{B}(\Xi^- \rightarrow \Lambda^0 e^- \bar{\nu}_e)(\times 10^{-4})$	5.63 ± 0.31	1.21 ± 0.71	$5.47 \pm 0.15^\ddagger$	4.94 ± 0.14
$\mathcal{B}(\Xi^0 \rightarrow \Sigma^+ e^- \bar{\nu}_e)(\times 10^{-4})$	2.52 ± 0.08	$2.52 \pm 0.08^\ddagger$	$2.52 \pm 0.08^\ddagger$	1.60 ± 0.06
$\mathcal{B}(\Lambda^0 \rightarrow p e^- \bar{\nu}_e)(\times 10^{-4})$	8.32 ± 0.14	$8.32 \pm 0.14^\ddagger$	$8.32 \pm 0.14^\ddagger$	6.05 ± 0.13
$\mathcal{B}(\Sigma^0 \rightarrow p e^- \bar{\nu}_e)(\times 10^{-13})$	\dots	2.41 ± 0.32	2.46 ± 0.32	2.01 ± 0.26
$\mathcal{B}(\Sigma^- \rightarrow n e^- \bar{\nu}_e)(\times 10^{-3})$	1.017 ± 0.034	$1.017 \pm 0.034^\ddagger$	$1.013 \pm 0.030^\ddagger$	0.851 ± 0.034
$\mathcal{B}(\Xi^- \rightarrow \Sigma^0 \mu^- \bar{\nu}_\mu)(\times 10^{-6})$	≤ 800	1.08 ± 0.09	1.13 ± 0.08	0.57 ± 0.04
$\mathcal{B}(\Xi^- \rightarrow \Lambda^0 \mu^- \bar{\nu}_\mu)(\times 10^{-4})$	$3.5_{-2.2}^{+3.5}$	0.33 ± 0.19	1.58 ± 0.04	1.41 ± 0.04
$\mathcal{B}(\Xi^0 \rightarrow \Sigma^+ \mu^- \bar{\nu}_\mu)(\times 10^{-6})$	2.33 ± 0.35	2.14 ± 0.14	2.18 ± 0.1	1.09 ± 0.08
$\mathcal{B}(\Lambda^0 \rightarrow p \mu^- \bar{\nu}_\mu)(\times 10^{-4})$	1.57 ± 0.35	1.35 ± 0.02	1.40 ± 0.02	0.94 ± 0.02
$\mathcal{B}(\Sigma^0 \rightarrow p \mu^- \bar{\nu}_\mu)(\times 10^{-13})$	\dots	1.05 ± 0.14	1.13 ± 0.15	0.92 ± 0.12
$\mathcal{B}(\Sigma^- \rightarrow n \mu^- \bar{\nu}_\mu)(\times 10^{-4})$	4.5 ± 0.4	4.53 ± 0.15	$4.76 \pm 0.14^\ddagger$	3.99 ± 0.17
$\mathcal{B}(\Sigma^- \rightarrow \Sigma^0 e^- \bar{\nu}_e)(\times 10^{-10})$	\dots	$4.36 \pm 4.01^\dagger$	$1.35 \pm 0.28^\dagger$	$1.11 \pm 0.23^\dagger$
$\mathcal{B}(\Sigma^- \rightarrow \Lambda^0 e^- \bar{\nu}_e)(\times 10^{-5})$	5.73 ± 0.27	$5.73 \pm 0.27^\ddagger$	$5.73 \pm 0.27^\ddagger$	3.18 ± 0.15
$\mathcal{B}(\Sigma^0 \rightarrow \Sigma^+ e^- \bar{\nu}_e)(\times 10^{-20})$	\dots	$3.41 \pm 3.20^\dagger$	$0.97 \pm 0.35^\dagger$	$0.80 \pm 0.28^\dagger$
$\mathcal{B}(\Sigma^+ \rightarrow \Lambda^0 e^+ \nu_e)(\times 10^{-5})$	2.0 ± 0.5	1.88 ± 0.11	1.86 ± 0.11	1.04 ± 0.06
$\mathcal{B}(\Xi^- \rightarrow \Xi^0 e^- \bar{\nu}_e)(\times 10^{-9})$	$\leq 2.3 \times 10^6$	$2.57 \pm 2.53^\dagger$	$0.42 \pm 0.24^\dagger$	$0.37 \pm 0.21^\dagger$
$\mathcal{B}(n \rightarrow p e^- \bar{\nu}_e)$	100%	100% ‡	100% ‡	(58.38 \pm 0.03)%

B. $T_{10} \rightarrow T_8 \ell^- \bar{\nu}_\ell$ semileptonic decays

The feynman diagram for $T_{10} \rightarrow T_8 \ell^- \bar{\nu}_\ell$ decays is also shown in Fig. 1. Similar to $T_{8A} \rightarrow T_{8B} \ell^- \bar{\nu}_\ell$ semileptonic decays, the SU(3) IRA helicity amplitudes $H_{\lambda_B \lambda_W}^{V(A)}$ for $T_{10} \rightarrow T_8 \ell^- \bar{\nu}_\ell$ decays can be parameterized as

$$H_{\lambda_B \lambda_W}^{V(A), IRA} = b_{n1} H(3)_n^k (T_{10})^{nij} (T_8)_{[ik]j}, \quad (13)$$

with $b_{n1} \equiv (b_{n1})_{\lambda_B \lambda_W}^{V(A)}(q^2)$. The helicity amplitudes $H_{\lambda_B \lambda_W}^{V(A)}$ for different $T_{10} \rightarrow T_8 \ell^- \bar{\nu}_\ell$ decays are given in Tab. IV. And the differential branching ratios of $T_{10A} \rightarrow T_{8B} \ell^- \bar{\nu}_\ell$ decays can be written as

$$\frac{d\mathcal{B}(T_{10A} \rightarrow T_{8B} \ell^- \bar{\nu}_\ell)}{dq^2} = \frac{G_F^2 |V_{uqn}|^2 \tau_A |\vec{p}_B| q^2}{384 \pi^3 m_A^2} \left(1 - \frac{m_\ell^2}{q^2}\right)^2 \left[B'_1 + \frac{m_\ell^2}{2q^2} B'_2\right], \quad (14)$$

with

$$B'_1 = \left|H_{\frac{1}{2}0}\right|^2 + \left|H_{-\frac{1}{2}0}\right|^2 + \left|H_{\frac{1}{2}1}\right|^2 + \left|H_{-\frac{1}{2}1}\right|^2 + \left|H_{-\frac{1}{2}-1}\right|^2 + \left|H_{\frac{1}{2}-1}\right|^2,$$

$$B'_2 = \left| H_{\frac{1}{2}0} \right|^2 + \left| H_{-\frac{1}{2}0} \right|^2 + \left| H_{\frac{1}{2}1} \right|^2 + \left| H_{-\frac{1}{2}1} \right|^2 + \left| H_{-\frac{1}{2}-1} \right|^2 + \left| H_{\frac{1}{2}-1} \right|^2 + 3 \left(\left| H_{\frac{1}{2}t} \right|^2 + \left| H_{-\frac{1}{2}t} \right|^2 \right). \quad (15)$$

The S_1 case given in Sec. II A will be considered in $T_{10} \rightarrow T_8 \ell^- \bar{\nu}_\ell$ semileptonic decays, where the $SU(3)_f$ parameters $(b_{n1})_{\lambda_B \lambda_W}^{V(A)}(q^2)$ are treated as constant without q^2 -dependence. The only parameter is b_{31} for $s \rightarrow u \ell^- \bar{\nu}_\ell$ transition and b_{21} for $d \rightarrow u e^- \bar{\nu}_e$ transition, respectively.

For $s \rightarrow u \ell^- \bar{\nu}_\ell$ transition, only $\mathcal{B}(\Omega^- \rightarrow \Xi^0 e^- \bar{\nu}_e)$ has been measured. The experimental datum is listed in the second column of Tab. V. We use $\mathcal{B}(\Omega^- \rightarrow \Xi^0 e^- \bar{\nu}_e)$ to constrain b_{31} , and then give the predictions for other relevant decay branching ratios. The results are given in the third column of Tab. V. We obtain $\mathcal{B}(\Omega^- \rightarrow \Xi^0 \mu^- \bar{\nu}_\mu) = (3.7 \pm 1.8) \times 10^{-3}$, which is very promising to be measured by the BESIII and LHCb. For $d \rightarrow u e^- \bar{\nu}_e$ transition, no decay mode has been measured yet. We use $H(\Omega^- \rightarrow \Xi^0 e^- \bar{\nu}_e) = H(\Delta^- \rightarrow n e^- \bar{\nu}_e)$ by the U-spin symmetry, *i.e.* $b_{21} = -b_{31}$, to predict the branching ratios of $d \rightarrow u e^- \bar{\nu}_e$ transition, which are listed in the third column of Tab. V, too. In Tab. V, all branching ratios except for $\mathcal{B}(\Omega^- \rightarrow \Xi^0 e^- \bar{\nu}_e, \Xi^0 \mu^- \bar{\nu}_\mu)$ are in the range of $10^{-16} - 10^{-15}$, since the life times of the $\Xi^{*0,-}$, $\Sigma^{*0,-}$ and $\Delta^{0,-}$ baryons are very small.

TABLE IV: The helicity amplitudes $H_{\lambda_B \lambda_W}^{V(A)}$ of $T_{10} \rightarrow T_8 \ell^- \bar{\nu}_\ell$ decays.

$H_{\lambda_B \lambda_W}^{V(A)}$	SU(3) IRA amplitudes
$s \rightarrow u \ell^- \bar{\nu}_\ell :$	
$H(\Omega^- \rightarrow \Xi^0 \ell^- \bar{\nu}_\ell)$	b_{31}
$3\sqrt{2}H(\Xi^{*-} \rightarrow \Lambda^0 \ell^- \bar{\nu}_\ell)$	$3b_{31}$
$\sqrt{6}H(\Xi^{*-} \rightarrow \Sigma^0 \ell^- \bar{\nu}_\ell)$	b_{31}
$\sqrt{3}H(\Xi^{*0} \rightarrow \Sigma^+ \ell^- \bar{\nu}_\ell)$	b_{31}
$\sqrt{3}H(\Sigma^{*-} \rightarrow n \ell^- \bar{\nu}_\ell)$	$-b_{31}$
$\sqrt{6}H(\Sigma^{*0} \rightarrow p \ell^- \bar{\nu}_\ell)$	$-b_{31}$
$d \rightarrow u e^- \bar{\nu}_e :$	
$\sqrt{3}H(\Xi^{*-} \rightarrow \Xi^0 e^- \bar{\nu}_e)$	b_{21}
$2\sqrt{3}H(\Sigma^{*-} \rightarrow \Lambda^0 e^- \bar{\nu}_e)$	$3b_{21}$
$\sqrt{6}H(\Sigma^{*-} \rightarrow \Sigma^0 e^- \bar{\nu}_e)$	b_{21}
$\sqrt{6}H(\Sigma^{*0} \rightarrow \Sigma^+ e^- \bar{\nu}_e)$	b_{21}
$H(\Delta^- \rightarrow n e^- \bar{\nu}_e)$	$-b_{21}$
$\sqrt{3}H(\Delta^0 \rightarrow p e^- \bar{\nu}_e)$	$-b_{21}$

TABLE V: The experimental data and the SU(3) IRA predictions with the $\pm 1\sigma$ error bar of $\mathcal{B}(T_{10} \rightarrow T_8 \ell^- \bar{\nu}_\ell)$.

Observables	Exp. Data [1]	S_1
$\mathcal{B}(\Omega^- \rightarrow \Xi^0 e^- \bar{\nu}_e)(\times 10^{-3})$	5.6 ± 2.8	$5.6 \pm 2.8^\ddagger$
$\mathcal{B}(\Xi^{*-} \rightarrow \Lambda^0 e^- \bar{\nu}_e)(\times 10^{-15})$...	6.6 ± 4.1
$\mathcal{B}(\Xi^{*-} \rightarrow \Sigma^0 e^- \bar{\nu}_e)(\times 10^{-15})$...	2.2 ± 1.4
$\mathcal{B}(\Xi^{*0} \rightarrow \Sigma^+ e^- \bar{\nu}_e)(\times 10^{-15})$...	1.6 ± 0.9
$\mathcal{B}(\Sigma^{*-} \rightarrow n e^- \bar{\nu}_e)(\times 10^{-15})$...	1.6 ± 0.9
$\mathcal{B}(\Sigma^{*0} \rightarrow p e^- \bar{\nu}_e)(\times 10^{-16})$...	9.3 ± 5.5
$\mathcal{B}(\Omega^- \rightarrow \Xi^0 \mu^- \bar{\nu}_\mu)(\times 10^{-3})$...	3.7 ± 1.8
$\mathcal{B}(\Xi^{*-} \rightarrow \Lambda^0 \mu^- \bar{\nu}_\mu)(\times 10^{-15})$...	4.9 ± 3.0
$\mathcal{B}(\Xi^{*-} \rightarrow \Sigma^0 \mu^- \bar{\nu}_\mu)(\times 10^{-15})$...	1.6 ± 1.0
$\mathcal{B}(\Xi^{*0} \rightarrow \Sigma^+ \mu^- \bar{\nu}_\mu)(\times 10^{-15})$...	1.0 ± 0.5
$\mathcal{B}(\Sigma^{*-} \rightarrow n \mu^- \bar{\nu}_\mu)(\times 10^{-15})$...	1.2 ± 0.7
$\mathcal{B}(\Sigma^{*0} \rightarrow p \mu^- \bar{\nu}_\mu)(\times 10^{-16})$...	7.1 ± 4.2
$\mathcal{B}(\Xi^{*-} \rightarrow \Xi^0 e^- \bar{\nu}_e)(\times 10^{-15})$...	3.6 ± 2.2
$\mathcal{B}(\Sigma^{*-} \rightarrow \Lambda^0 e^- \bar{\nu}_e)(\times 10^{-15})$...	6.2 ± 3.3
$\mathcal{B}(\Sigma^{*-} \rightarrow \Sigma^0 e^- \bar{\nu}_e)(\times 10^{-16})$...	2.7 ± 1.4
$\mathcal{B}(\Sigma^{*0} \rightarrow \Sigma^+ e^- \bar{\nu}_e)(\times 10^{-16})$...	3.1 ± 1.8
$\mathcal{B}(\Delta^- \rightarrow n e^- \bar{\nu}_e)(\times 10^{-15})$...	4.9 ± 2.6
$\mathcal{B}(\Delta^0 \rightarrow p e^- \bar{\nu}_e)(\times 10^{-15})$...	1.7 ± 0.9

III. Nonleptonic two-body decays of light baryons

In this section, we discuss the two-body nonleptonic decays of light baryons $T_{8,10} \rightarrow T_8 M_8$, where M_8 are light pseudoscalar P and vector V meson octets under the $SU(3)$ flavor symmetry of u, d, s quarks

$$P_8 = \begin{pmatrix} \frac{\eta_8}{\sqrt{6}} + \frac{\pi^0}{\sqrt{2}} & \pi^+ & K^+ \\ \pi^- & \frac{\eta_8}{\sqrt{6}} - \frac{\pi^0}{\sqrt{2}} & K^0 \\ K^- & \bar{K}^0 & -\sqrt{\frac{2}{3}}\eta_8 \end{pmatrix}, \quad (16)$$

$$V_8 = \begin{pmatrix} \frac{\omega_8}{\sqrt{6}} + \frac{\rho^0}{\sqrt{2}} & \rho^+ & K^{*+} \\ \rho^- & \frac{\omega_8}{\sqrt{6}} - \frac{\rho^0}{\sqrt{2}} & K^{*0} \\ K^{*-} & \bar{K}^{*0} & -\sqrt{\frac{2}{3}}\omega_8 \end{pmatrix}. \quad (17)$$

A. Weak decays of light baryons

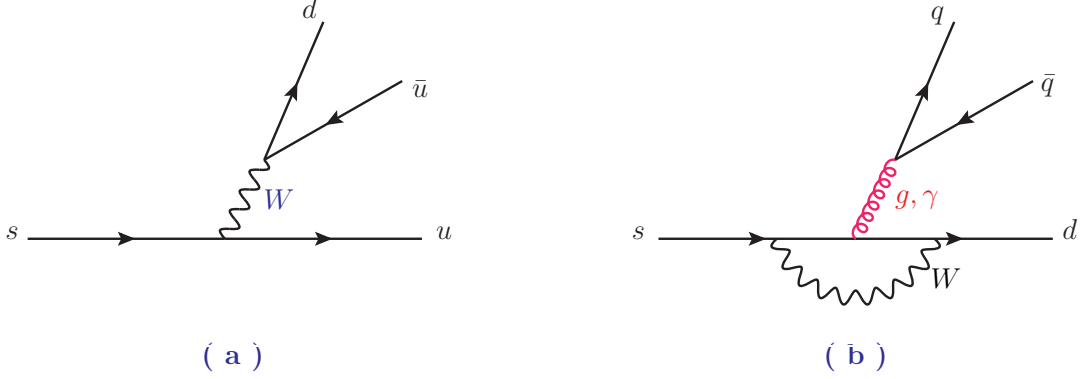


FIG. 2: Feynman diagrams for the s quark decays in the SM.

In the SM, as shown in Fig. 2, there are two kinds of diagrams for the nonleptonic s quark decays, the tree level diagram in Fig. 2 (a) and the penguin diagram in Fig. 2 (b). The effective Hamiltonian for nonleptonic s quark decays at scales $\mu < m_c$ can be written as [55]

$$\mathcal{H}_{eff} = \frac{G_F}{\sqrt{2}} V_{ud} V_{us}^* \sum_{i=1}^{10} \left[z_i(\mu) - \frac{V_{td} V_{ts}^*}{V_{ud} V_{us}^*} y_i(\mu) \right] Q_i(\mu), \quad (18)$$

where V_{uq} is the CKM matrix element, $z_i(\mu)$ and $y_i(\mu)$ are Wilson coefficients. The four-quark operators Q_i are

$$\begin{aligned} Q_1 &= (\bar{d}_\alpha u_\beta)_{V-A} (\bar{u}_\beta s_\alpha)_{V-A}, & Q_2 &= (\bar{d}u)_{V-A} (\bar{u}s)_{V-A}, \\ Q_{3,5} &= (\bar{d}s)_{V-A} \sum_{q=u,d,s} (\bar{q}q)_{V\mp A}, & Q_{4,6} &= (\bar{d}_\beta s_\alpha)_{V-A} \sum_{q=u,d,s} (\bar{q}_\alpha q_\beta)_{V\mp A}, \\ Q_{7,9} &= \frac{3}{2} (\bar{d}s)_{V-A} \sum_{q=u,d,s} e_q (\bar{q}q)_{V\pm A}, & Q_{8,10} &= \frac{3}{2} (\bar{d}_\beta s_\alpha)_{V-A} \sum_{q=u,d,s} e_q (\bar{q}_\alpha q_\beta)_{V\pm A}, \end{aligned} \quad (19)$$

where $Q_{1,2}$ are current-current operators corresponding to Fig. 2 (a), Q_{3-6} (Q_{7-10}) are QCD (electroweak) penguin operators corresponding to Fig. 2 (b). In Eq. (18), the magnetic penguin operators are ignored since their contributions are small. $C_i(\mu) \equiv z_i(\mu) - \frac{V_{td} V_{ts}^*}{V_{ud} V_{us}^*} y_i(\mu)$ at $\mu = 1$ GeV on $\Lambda_{\overline{MS}}^{(4)}$ in the NDR scheme are [55]

$$\begin{aligned} C_1 &= -0.625, & C_2 &= 1.361, & C_3 &= 0.023, & C_4 &= -0.058, & C_5 &= 0.009, & C_6 &= -0.059, \\ C_7/\alpha_e &= 0.021, & C_8/\alpha_e &= 0.027, & C_9/\alpha_e &= 0.036, & C_{10}/\alpha_e &= -0.015. \end{aligned} \quad (20)$$

Compared with tree-level contributions related to $C_{1,2}$, the penguin contributions are suppressed by smaller Wilson coefficients $C_{3,\dots,10}$ and can be ignored in these decays.

The four-quark operators Q_i can be rewritten as $(\bar{q}_i q^k)(\bar{q}_j s)$ with $q_i = (u, d)$ as the doublet of 2 under the SU(2) symmetry by omitting the Lorentz-Dirac structure. Since $(\bar{q}_i q^k)(\bar{q}_j s)$ can be decomposed as the irreducible representations (IR) of $(\bar{2} \otimes 2 \otimes 2)s = (\bar{2}_p \oplus \bar{2}_t \oplus 4)s$, one may obtain that

$$\begin{aligned} \mathcal{O}(\bar{2}_p)_2 &= (\bar{u}u)(\bar{d}s) + (\bar{d}d)(\bar{d}s), \\ \mathcal{O}(\bar{2}_t)_2 &= (\bar{d}u)(\bar{u}s) + (\bar{d}d)(\bar{d}s), \\ \mathcal{O}(4)_{12}^1 &= \frac{1}{3}(\bar{u}u)(\bar{d}s) - \frac{1}{3}(\bar{d}d)(\bar{d}s) + \frac{1}{3}(\bar{d}u)(\bar{u}s), \end{aligned} \quad (21)$$

and we have the relation $\mathcal{O}(4)_{21}^1 = -\mathcal{O}(4)_{22}^2 = \mathcal{O}(4)_{12}^1$ by the traceless condition. Then $Q_{1,2}$, Q_{3-6} and $Q_{7,10}$ can be transformed under SU(2) symmetry as $\bar{2}_p \oplus \bar{2}_t \oplus 4$, $\bar{2}_p/\bar{2}_t$ and $\bar{2}_p \oplus \bar{2}_t \oplus 4$, respectively,

$$\begin{aligned}
Q_1 &= \mathcal{O}(4)_{12}^1 + \frac{2}{3}\mathcal{O}(\bar{2}_p)_2 - \frac{1}{3}\mathcal{O}(\bar{2}_t)_2, \\
Q_2 &= \mathcal{O}(4)_{12}^1 - \frac{1}{3}\mathcal{O}(\bar{2}_p)_2 + \frac{2}{3}\mathcal{O}(\bar{2}_t)_2, \\
Q_3 &= \mathcal{O}(\bar{2}_p)_2, & Q_4 &= \mathcal{O}(\bar{2}_t)_2, \\
Q_5 &= \mathcal{O}'(\bar{2}_p)_2, & Q_6 &= \mathcal{O}'(\bar{2}_t)_2, \\
Q_7 &= \frac{3}{2}\mathcal{O}'(4)_{12}^1 + \frac{1}{2}\mathcal{O}'(\bar{2}_p)_2 - \frac{1}{2}\mathcal{O}'(\bar{2}_t)_2, \\
Q_8 &= \frac{3}{2}\mathcal{O}'(4)_{12}^1 - \frac{1}{2}\mathcal{O}'(\bar{2}_p)_2 + \frac{1}{2}\mathcal{O}'(\bar{2}_t)_2, \\
Q_9 &= \frac{3}{2}\mathcal{O}(4)_{12}^1 + \frac{1}{2}\mathcal{O}(\bar{2}_p)_2 - \frac{1}{2}\mathcal{O}(\bar{2}_t)_2, \\
Q_{10} &= \frac{3}{2}\mathcal{O}(4)_{12}^1 - \frac{1}{2}\mathcal{O}(\bar{2}_p)_2 + \frac{1}{2}\mathcal{O}(\bar{2}_t)_2,
\end{aligned} \tag{22}$$

where $\mathcal{O}'(\bar{2}_p)_2$, $\mathcal{O}'(\bar{2}_t)_2$ and $\mathcal{O}'(4)_{12}^1$ are operators related to $Q_{5,6,7,8}$, which have the same SU(3) structure as $\mathcal{O}(\bar{2}_p)_2$, $\mathcal{O}(\bar{2}_t)_2$ and $\mathcal{O}(4)_{12}^1$ but different Lorentz-Dirac structures.

By using the bases of the SU(2) symmetry, the effective Hamiltonian in Eq. (18) can be transformed as

$$\mathcal{H}_{eff}^{IR} = \frac{G_F}{\sqrt{2}} V_{ud} V_{us}^* \left[\bar{C}_4 \mathcal{O}(4)_{12}^1 + \bar{C}_{\bar{2}_p} \mathcal{O}(\bar{2}_p)_2 + \bar{C}_{\bar{2}_t} \mathcal{O}(\bar{2}_t)_2 + \bar{C}'_4 \mathcal{O}'(4)_{12}^1 + \bar{C}'_{\bar{2}_p} \mathcal{O}'(\bar{2}_p)_2 + \bar{C}'_{\bar{2}_t} \mathcal{O}'(\bar{2}_t)_2 \right], \tag{23}$$

with

$$\begin{aligned}
\bar{C}_4 &= C_1 + C_2 + \frac{3}{2}(C_9 + C_{10}), \\
\bar{C}_{\bar{2}_p} &= \frac{2}{3}C_1 - \frac{1}{3}C_2 + C_3 + \frac{1}{2}(C_9 - C_{10}), \\
\bar{C}_{\bar{2}_t} &= -\frac{1}{3}C_1 + \frac{2}{3}C_2 + C_4 - \frac{1}{2}(C_9 - C_{10}), \\
\bar{C}'_4 &= \frac{3}{2}(C_7 + C_8), \\
\bar{C}'_{\bar{2}_p} &= C_5 + \frac{1}{2}(C_7 - C_8), \\
\bar{C}'_{\bar{2}_t} &= C_6 - \frac{1}{2}(C_7 - C_8).
\end{aligned} \tag{24}$$

From Eq. (20), one can see that the contributions from current-current operators related to $C_{1,2}$ are much larger than others related to $C_{3,\dots,10}$. So we will only consider current-current operator contributions in the following analysis. After neglecting $C_{3,\dots,10}$, the effective Hamiltonian in Eq. (23) can be rewritten as

$$\mathcal{H}_{eff}^{IR} = \frac{G_F}{\sqrt{2}} V_{ud} V_{us}^* \left\{ C_+ \left[2H(4) + \frac{1}{3}(H(\bar{2}_t) + H(\bar{2}_p)) \right] + C_- (H(\bar{2}_t) - H(\bar{2}_p)) \right\}, \tag{25}$$

where $C_{\pm} \equiv (C_2 \pm C_1)/2$, and H_k^{ij} is related to $(\bar{q}_i q^k)(\bar{q}_j s)$ operators. From Eq. (20), one gets $C_+^2/C_-^2 \approx 13.7\%$, so C_- term related to $H(\bar{2}_t) - H(\bar{2}_p)$ gives the dominant contribution to the decay branching ratios. The non-zero entries of H_k^{ij} corresponding to current-current operators in SU(2) flavor space are

$$H(\bar{2}_p)^2 = H(\bar{2}_t)^2 = 1, \quad H(4)_1^{12} = H(4)_1^{21} = \frac{1}{3}. \tag{26}$$

Noted that $H(4)_2^{22} = -\frac{1}{3}$ only contributes to the penguin operators and we ignore it.

In Eq. (25), the $\bar{2}$ irreducible representation is linear combinations of $\bar{2}_{p,t}$, so we need only consider a single $\bar{2}$ when computing amplitudes from the invariants and reduced matrix elements [25].

The amplitudes of the $T_{8,10} \rightarrow T_8 M_8$ decays can be written via the effective Hamiltonian in Eq. (18) as

$$A(T_{8,10} \rightarrow T_8 M_8) = \langle T_8 M_8 | \mathcal{H}_{eff} | T_{8,10} \rangle. \quad (27)$$

These amplitudes may be divided into the S wave and P wave amplitudes, which have been analysed, for instance, in heavy baryon chiral perturbation theory [56–59] and by using a relativistic chiral unitary approach based on coupled channels [60]. Moreover, since \mathcal{H}_{eff}^{IR} is irreducible in the SU(2) symmetry, and the initial and final state baryons (T_8 , T_{10} , M_8) are irreducible in the SU(3) symmetry, the amplitudes of $T_{8,10} \rightarrow T_8 M_8$ can be further written as

$$A(T_{8,10} \rightarrow T_8 M_8) = \langle T_8 M_8 | \mathcal{H}_{eff}^{IR} | T_{8,10} \rangle = A(\mathcal{O}_4) + A(\mathcal{O}_2). \quad (28)$$

1. $T_8 \rightarrow T_8 M_8$ weak decays

Following Ref. [36], the Feynman diagrams for $T_8 \rightarrow T_8 M_8$ nonleptonic s quark decays are displayed in Fig. 3, and the SU(3) IRA amplitudes are

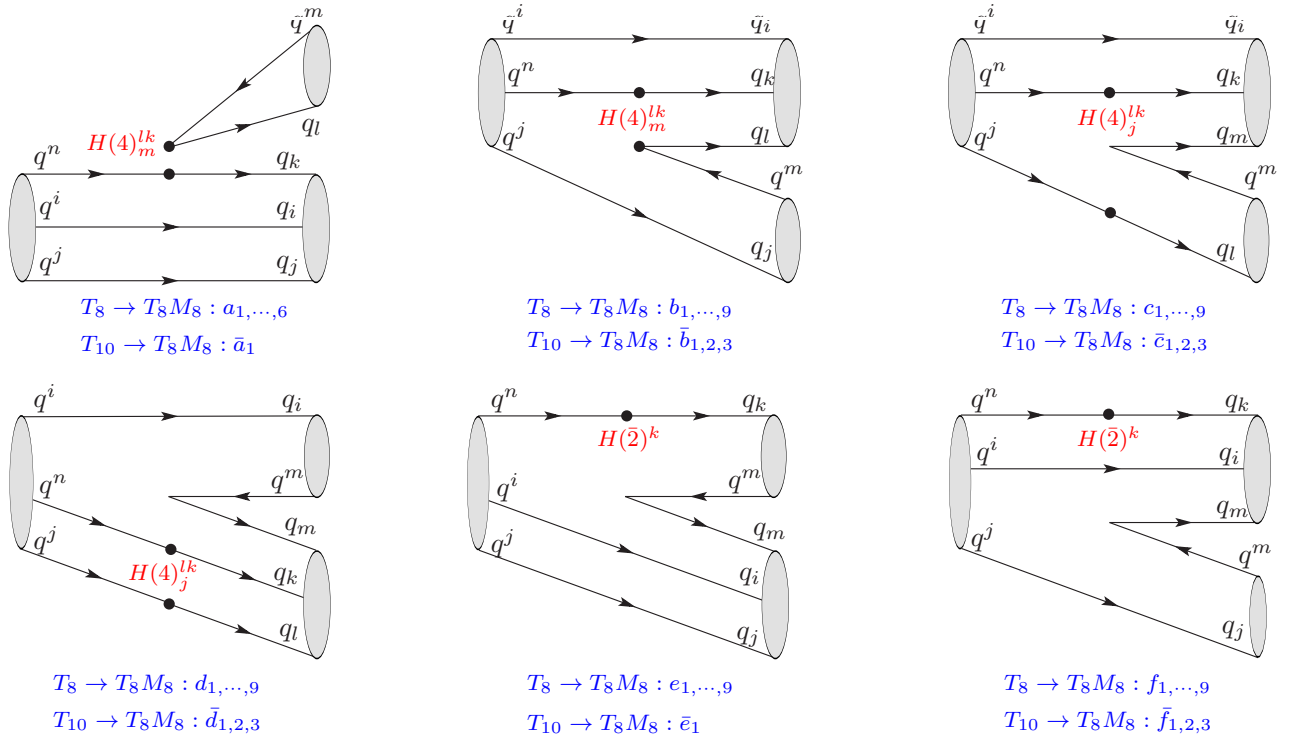


FIG. 3: Feynman diagrams of IRA for $T_{8,10} \rightarrow T_8 M_8$ nonleptonic two-body decays with $q^n = s$.

$$\begin{aligned}
A(T_8 \rightarrow T_8 M_8)^{IRA} = & a_1 H(4)_m^{lk}(T_8)^{[ij]n}(T_8)_{[ij]k}(M_8)_l^m + a_2 H(4)_m^{lk}(T_8)^{[ij]n}(T_8)_{[ik]j}(M_8)_l^m + a_3 H(4)_m^{lk}(T_8)^{[ij]n}(T_8)_{[jk]i}(M_8)_l^m \\
& + a_4 H(4)_m^{lk}(T_8)^{[in]j}(T_8)_{[ij]k}(M_8)_l^m + a_5 H(4)_m^{lk}(T_8)^{[in]j}(T_8)_{[ik]j}(M_8)_l^m + a_6 H(4)_m^{lk}(T_8)^{[in]j}(T_8)_{[jk]i}(M_8)_l^m \\
& + a_7 H(4)_m^{lk}(T_8)^{[jn]i}(T_8)_{[ij]k}(M_8)_l^m + a_8 H(4)_m^{lk}(T_8)^{[jn]i}(T_8)_{[ik]j}(M_8)_l^m + a_9 H(4)_m^{lk}(T_8)^{[jn]i}(T_8)_{[jk]i}(M_8)_l^m \\
& + b_1 H(4)_m^{lk}(T_8)^{[ij]n}(T_8)_{[il]k}(M_8)_j^m + b_2 H(4)_m^{lk}(T_8)^{[ij]n}(T_8)_{[kl]i}(M_8)_j^m + b_3 H(4)_m^{lk}(T_8)^{[ij]n}(T_8)_{[ki]l}(M_8)_j^m \\
& + b_4 H(4)_m^{lk}(T_8)^{[in]j}(T_8)_{[il]k}(M_8)_j^m + b_5 H(4)_m^{lk}(T_8)^{[in]j}(T_8)_{[kl]i}(M_8)_j^m + b_6 H(4)_m^{lk}(T_8)^{[in]j}(T_8)_{[ki]l}(M_8)_j^m \\
& + b_7 H(4)_m^{lk}(T_8)^{[jn]i}(T_8)_{[il]k}(M_8)_j^m + b_8 H(4)_m^{lk}(T_8)^{[jn]i}(T_8)_{[kl]i}(M_8)_j^m + b_9 H(4)_m^{lk}(T_8)^{[jn]i}(T_8)_{[ki]l}(M_8)_j^m \\
& + c_1 H(4)_j^{lk}(T_8)^{[ij]n}(T_8)_{[ki]m}(M_8)_l^m + c_2 H(4)_j^{lk}(T_8)^{[ij]n}(T_8)_{[km]i}(M_8)_l^m + c_3 H(4)_j^{lk}(T_8)^{[ij]n}(T_8)_{[im]k}(M_8)_l^m \\
& + c_4 H(4)_j^{lk}(T_8)^{[in]j}(T_8)_{[ki]m}(M_8)_l^m + c_5 H(4)_j^{lk}(T_8)^{[in]j}(T_8)_{[km]i}(M_8)_l^m + c_6 H(4)_j^{lk}(T_8)^{[in]j}(T_8)_{[im]k}(M_8)_l^m \\
& + c_7 H(4)_j^{lk}(T_8)^{[jn]i}(T_8)_{[ki]m}(M_8)_l^m + c_8 H(4)_j^{lk}(T_8)^{[jn]i}(T_8)_{[km]i}(M_8)_l^m + c_9 H(4)_j^{lk}(T_8)^{[jn]i}(T_8)_{[im]k}(M_8)_l^m \\
& + d_1 H(4)_j^{lk}(T_8)^{[ij]n}(T_8)_{[mk]l}(M_8)_i^m + d_2 H(4)_j^{lk}(T_8)^{[ij]n}(T_8)_{[ml]k}(M_8)_i^m + d_3 H(4)_j^{lk}(T_8)^{[ij]n}(T_8)_{[kl]m}(M_8)_i^m \\
& + d_4 H(4)_j^{lk}(T_8)^{[in]j}(T_8)_{[mk]l}(M_8)_i^m + d_5 H(4)_j^{lk}(T_8)^{[in]j}(T_8)_{[ml]k}(M_8)_i^m + d_6 H(4)_j^{lk}(T_8)^{[in]j}(T_8)_{[kl]m}(M_8)_i^m \\
& + d_7 H(4)_j^{lk}(T_8)^{[jn]i}(T_8)_{[mk]l}(M_8)_i^m + d_8 H(4)_j^{lk}(T_8)^{[jn]i}(T_8)_{[ml]k}(M_8)_i^m + d_9 H(4)_j^{lk}(T_8)^{[jn]i}(T_8)_{[kl]m}(M_8)_i^m \\
& + e_1 H(\bar{2})^k(T_8)^{[ij]n}(T_8)_{[ij]m}(M_8)_k^m + e_2 H(\bar{2})^k(T_8)^{[ij]n}(T_8)_{[im]j}(M_8)_k^m + e_3 H(\bar{2})^k(T_8)^{[ij]n}(T_8)_{[jm]i}(M_8)_k^m \\
& + e_4 H(\bar{2})^k(T_8)^{[in]j}(T_8)_{[ij]m}(M_8)_k^m + e_5 H(\bar{2})^k(T_8)^{[in]j}(T_8)_{[im]j}(M_8)_k^m + e_6 H(\bar{2})^k(T_8)^{[in]j}(T_8)_{[jm]i}(M_8)_k^m \\
& + e_7 H(\bar{2})^k(T_8)^{[jn]i}(T_8)_{[ij]m}(M_8)_k^m + e_8 H(\bar{2})^k(T_8)^{[jn]i}(T_8)_{[im]j}(M_8)_k^m + e_9 H(\bar{2})^k(T_8)^{[jn]i}(T_8)_{[jm]i}(M_8)_k^m \\
& + f_1 H(\bar{2})^k(T_8)^{[ij]n}(T_8)_{[ki]m}(M_8)_j^m + f_2 H(\bar{2})^k(T_8)^{[ij]n}(T_8)_{[km]i}(M_8)_j^m + f_3 H(\bar{2})^k(T_8)^{[ij]n}(T_8)_{[im]k}(M_8)_j^m \\
& + f_4 H(\bar{2})^k(T_8)^{[in]j}(T_8)_{[ki]m}(M_8)_j^m + f_5 H(\bar{2})^k(T_8)^{[in]j}(T_8)_{[km]i}(M_8)_j^m + f_6 H(\bar{2})^k(T_8)^{[in]j}(T_8)_{[im]k}(M_8)_j^m \\
& + f_7 H(\bar{2})^k(T_8)^{[jn]i}(T_8)_{[ki]m}(M_8)_j^m + f_8 H(\bar{2})^k(T_8)^{[jn]i}(T_8)_{[km]i}(M_8)_j^m + f_9 H(\bar{2})^k(T_8)^{[jn]i}(T_8)_{[im]k}(M_8)_j^m,
\end{aligned} \tag{29}$$

where the coefficients $a_i, b_i, c_i, d_i, e_i, f_i$ are constants which contain the Wilson coefficients, CKM matrix elements and information about QCD dynamics. Using $H(4)_c^{ab}$ is symmetric in upper indices, b_i and d_i terms can be simplified by

$$\begin{aligned}
b_3 = -b_1, \quad b_6 = -b_4, \quad b_9 = -b_7, \quad b_2 = b_5 = b_8 = 0, \\
d_2 = d_1, \quad d_5 = d_4, \quad d_8 = d_7, \quad d_3 = d_6 = d_9 = 0.
\end{aligned} \tag{30}$$

In addition, using i, j antisymmetric in $T_8^{[ij]n}$ and i, j indices are arbitrary in e_i terms, we have

$$a_3 = -a_2, \quad a_7 = -a_4, \quad a_8 = a_6, \quad a_9 = a_5, \quad e_3 = -e_2, \quad e_7 = -e_4, \quad e_8 = e_6, \quad e_9 = e_5. \tag{31}$$

Finally, Eq. (32) can be simplified as

$$\begin{aligned}
A(T_8 \rightarrow T_8 M_8)^{IRA,J} = & a_1 H(4)_m^{lk}(T_8)^{[ij]n}(T_8)_{[ij]k}(M_8)_l^m + a_2 H(4)_m^{lk}(T_8)^{[ij]n}(T_8)_{[ik]j}(M_8)_l^m \\
& + a_4 H(4)_m^{lk}(T_8)^{[in]j}(T_8)_{[ij]k}(M_8)_l^m + a_5 H(4)_m^{lk}(T_8)^{[in]j}(T_8)_{[ik]j}(M_8)_l^m + a_6 H(4)_m^{lk}(T_8)^{[in]j}(T_8)_{[jk]i}(M_8)_l^m \\
& + b_1 H(4)_m^{lk}(T_8)^{[ij]n}(T_8)_{[il]k}(M_8)_j^m + b_4 H(4)_m^{lk}(T_8)^{[in]j}(T_8)_{[il]k}(M_8)_j^m + b_7 H(4)_m^{lk}(T_8)^{[jn]i}(T_8)_{[il]k}(M_8)_j^m \\
& + c_1 H(4)_j^{lk}(T_8)^{[ij]n}(T_8)_{[ki]m}(M_8)_l^m + c_2 H(4)_j^{lk}(T_8)^{[ij]n}(T_8)_{[km]i}(M_8)_l^m + c_3 H(4)_j^{lk}(T_8)^{[ij]n}(T_8)_{[im]k}(M_8)_l^m \\
& + c_4 H(4)_j^{lk}(T_8)^{[in]j}(T_8)_{[ki]m}(M_8)_l^m + c_5 H(4)_j^{lk}(T_8)^{[in]j}(T_8)_{[km]i}(M_8)_l^m + c_6 H(4)_j^{lk}(T_8)^{[in]j}(T_8)_{[im]k}(M_8)_l^m \\
& + c_7 H(4)_j^{lk}(T_8)^{[jn]i}(T_8)_{[ki]m}(M_8)_l^m + c_8 H(4)_j^{lk}(T_8)^{[jn]i}(T_8)_{[km]i}(M_8)_l^m + c_9 H(4)_j^{lk}(T_8)^{[jn]i}(T_8)_{[im]k}(M_8)_l^m
\end{aligned}$$

$$\begin{aligned}
& +d_1 H(4)_j^{lk} (T_8)^{[ij]n} (T_8)_{[mk]l} (M_8)_i^m + d_4 H(4)_j^{lk} (T_8)^{[in]j} (T_8)_{[mk]l} (M_8)_i^m + d_7 H(4)_j^{lk} (T_8)^{[jn]i} (T_8)_{[mk]l} (M_8)_i^m \\
& +e_1 H(\bar{2})^k (T_8)^{[ij]n} (T_8)_{[ij]m} (M_8)_k^m + e_2 H(\bar{2})^k (T_8)^{[ij]n} (T_8)_{[im]j} (M_8)_k^m \\
& +e_4 H(\bar{2})^k (T_8)^{[in]j} (T_8)_{[ij]m} (M_8)_k^m + e_5 H(\bar{2})^k (T_8)^{[in]j} (T_8)_{[im]j} (M_8)_k^m + e_6 H(\bar{2})^k (T_8)^{[in]j} (T_8)_{[jm]i} (M_8)_k^m \\
& +f_1 H(\bar{2})^k (T_8)^{[ij]n} (T_8)_{[ki]m} (M_8)_j^m + f_2 H(\bar{2})^k (T_8)^{[ij]n} (T_8)_{[km]i} (M_8)_j^m + f_3 H(\bar{2})^k (T_8)^{[ij]n} (T_8)_{[im]k} (M_8)_j^m \\
& +f_4 H(\bar{2})^k (T_8)^{[in]j} (T_8)_{[ki]m} (M_8)_j^m + f_5 H(\bar{2})^k (T_8)^{[in]j} (T_8)_{[km]i} (M_8)_j^m + f_6 H(\bar{2})^k (T_8)^{[in]j} (T_8)_{[im]k} (M_8)_j^m \\
& +f_7 H(\bar{2})^k (T_8)^{[jn]i} (T_8)_{[ki]m} (M_8)_j^m + f_8 H(\bar{2})^k (T_8)^{[jn]i} (T_8)_{[km]i} (M_8)_j^m + f_9 H(\bar{2})^k (T_8)^{[jn]i} (T_8)_{[im]k} (M_8)_j^m.
\end{aligned} \tag{32}$$

In Tab. VI, we list the IRA amplitudes of $T_8 \rightarrow T_8 P_8$ weak decays, which include the $H(4)_1^{12}$, $H(4)_2^{22}$ and $H(\bar{2})^2$ terms. The corresponding $T_8 \rightarrow T_8 V_8$ weak decays have the same relations as $T_8 \rightarrow T_8 P_8$ weak decays. If only considering the dominant contributions from $H(\bar{2})^2$ and redefining the parameters

$$\begin{aligned}
A_1 &= 2(e_5 + e_6) + (f_4 + f_5 + f_7 + f_8), \\
A_2 &= 2(e_5 + e_6) + (f_5 + f_6 + f_8 + f_9), \\
A_3 &= 2(e_5 + e_6) - (f_4 - f_5 + f_7 - f_8), \\
A_4 &= 4(e_1 + e_2 + e_4) + 2(e_5 - e_6) - (2f_1 + 2f_2 + f_4 + f_5 - f_7 - f_8), \\
A_5 &= 2(e_1 + e_2 + e_4 + 2e_5 + e_6) - (f_1 + 2f_2 + f_3) + (f_7 + 2f_8 + f_9),
\end{aligned} \tag{33}$$

the IRA amplitudes can be greatly simplified as listed in the last column of Tab. VI, in which we can easily see the relations of different decay amplitudes.

The branching ratios of $T_8 \rightarrow T_8 P_8$ can be written as

$$\mathcal{B}(T_{8A} \rightarrow T_{8B} P_8) = \frac{\tau_A |p_{cm}|}{8\pi m_A^2} |A(T_{8A} \rightarrow T_{8B} P_8)|^2. \tag{34}$$

For more accurate results, we will consider the mass difference in the amplitudes [61]

$$A(T_{8A} \rightarrow T_{8B} P_8) \propto \frac{m_A}{m_B} p_{cm} N_B N_A, \tag{35}$$

with

$$\begin{aligned}
p_{cm} &= \frac{1}{2m_A} \sqrt{(m_A^2 - (m_B + m_P)^2)(m_A^2 - (m_B - m_P)^2)}, \\
N_A &= \sqrt{2m_A}, \\
N_B &= \sqrt{\frac{(m_A + m_B)^2 - m_P^2}{2m_A}}.
\end{aligned} \tag{36}$$

The experimental measurements with the $\pm 1\sigma$ error bar of $T_8 \rightarrow T_8 P_8$ weak decays are listed in the second column of Tab. VII. There are four real parameters ($A_1, A_2 e^{i\phi_A}, A_3$) for five $\Sigma \rightarrow p\pi, n\pi$ decays, one can obtain $A_1 = 2.48 \pm 0.01$, $A_2 = 1.74 \pm 0.01$ and $|\phi_A| \leq 45.35^\circ$ by using the data of $\mathcal{B}(\Sigma^+ \rightarrow p\pi^0, n\pi^+, \Sigma^- \rightarrow n\pi^-)$, furthermore, $\mathcal{B}(\Sigma^0 \rightarrow p\pi^-)$ could be obtained in terms of A_1 . In addition, the five $\Sigma \rightarrow n\pi, p\pi$ decay modes also have the isospin relations

$$\begin{aligned}
A(\Sigma^+ \rightarrow p\pi^0) &= -\frac{\sqrt{2}}{3} (A_{\frac{1}{2}} - A_{\frac{3}{2}}), \\
A(\Sigma^+ \rightarrow n\pi^+) &= \frac{1}{3} (2A_{\frac{1}{2}} + A_{\frac{3}{2}}),
\end{aligned}$$

TABLE VI: The $SU(3)$ IRA amplitudes of $T_8 \rightarrow T_8 P$ weak decays.

Amplitudes	$H(4)_{11}^{12}$	$H(4)_{22}^{22}$	$H(\bar{2})^2$	Simplified Amplitudes
$\sqrt{2}A(\Sigma^+ \rightarrow p\pi^0)$	$-2(a_5 + a_6) - 2(b_4 + b_7) + (c_4 + 2c_5 + c_6) + (c_7 + 2c_8 + c_9) - 2(d_4 + d_7)$	$2(a_5 + a_6)$	$2(e_5 + e_6) + f_4 + f_5 + f_7 + f_8$	A_1
$A(\Sigma^+ \rightarrow n\pi^+)$	$(c_4 - c_6 + c_7 - c_9) + 2(d_4 + d_7)$	$-2(b_4 + b_7)$	$f_4 - f_6 + f_7 - f_9$	$A_1 - A_2$
$A(\Sigma^- \rightarrow n\pi^-)$	$-2(a_5 + a_6) - 2(b_4 + b_7)$	$-(c_5 + c_6 + c_8 + c_9) + 2(d_4 + d_7)$	$-2(e_5 + e_6) - (f_5 + f_6 + f_8 + f_9)$	$-A_2$
$\sqrt{2}A(\Sigma^0 \rightarrow p\pi^-)$	$2(a_5 + a_6) - 2(b_4 + b_7) - (c_4 - c_6 + c_7 - c_9) - 2(d_4 + d_7)$	$c_4 + c_5 + c_7 + c_8$	$2(e_5 + e_6) + f_4 + f_5 + f_7 + f_8$	A_1
$2A(\Sigma^0 \rightarrow n\pi^0)$	$-2(a_5 + a_6) + 2(b_4 + b_7) + (c_4 + 2c_5 + c_6) + (c_7 + 2c_8 + c_9) - 2(d_4 + d_7)$	$2(a_5 + a_6) + 2(b_4 + b_7) - (c_4 - c_6 + c_7 - c_9) - 2(d_4 + d_7)$	$2(e_5 + e_6) - (f_4 - f_5 + f_7 - f_8)$	A_3
$\sqrt{6}A(\Lambda^0 \rightarrow p\pi^-)$	$-4(a_1 + a_2 + a_4) - 2(a_5 - a_6) - 2(2b_1 + b_4 - b_7) + (2c_1 - 2c_3 + c_4 - c_6 - c_7 + c_9) + 2(2d_1 + d_4 - d_7)$	$2c_1 + 2c_2 + c_4 + c_5 - c_7 - c_8$	$-4(e_1 + e_2 + e_4) - 2(e_5 - e_6) + (2f_1 + 2f_2 + f_4 + f_5 - f_7 - f_8)$	$-A_4$
$2\sqrt{3}A(\Lambda^0 \rightarrow n\pi^0)$	$-4(a_1 + a_2 + a_4) - 2(a_5 - a_6) - 2(2b_1 + b_4 - b_7) - 2(c_1 + 2c_2 + c_3) - (c_4 + 2c_5 + c_6) + (c_7 + 2c_8 + c_9) + 2(2d_1 + d_4 - d_7)$	$4(a_1 + a_2 + a_4) + 2(a_5 - a_6) + 2(2b_1 + b_4 - b_7) - (2c_1 + 2c_3 - c_4 + c_6 + c_7 - c_9) - 2(2d_1 + d_4 - d_7)$	$4(e_1 + e_2 + e_4) + 2(e_5 - e_6) - (2f_1 + 2f_2 + f_4 + f_5 - f_7 - f_8)$	A_4
$\sqrt{6}A(\Xi^- \rightarrow \Lambda^0 \pi^-)$	$2(a_1 + a_2 + a_4 + 2a_5 + a_6)$	$-(c_1 + 2c_2 + c_3) + (c_7 + 2c_8 + c_9)$	$2(e_1 + e_2 + e_4 + 2e_5 + e_6) - (f_1 + 2f_2 + f_3) + (f_7 + 2f_8 + f_9)$	A_5
$2\sqrt{3}A(\Xi^0 \rightarrow \Lambda^0 \pi^0)$	$2(a_1 + a_2 + a_4 + 2a_5 + a_6) + 2(c_1 + 2c_2 + c_3) - 2(c_7 + 2c_8 + c_9)$	$-2(a_1 + a_2 + a_4 + 2a_5 + a_6)$	$-2(e_1 + e_2 + e_4 + 2e_5 + e_6) + (f_1 + 2f_2 + f_3) - (f_7 + 2f_8 + f_9)$	$-A_5$

TABLE VII: The experimental measurements and the SM predictions with the $\pm 1\sigma$ error bar of branching ratios of $T_8 \rightarrow T_8 P_8$ weak decays. † denotes which experimental data have been used to give the effective constraints of the parameters, ‡ denotes the predictions depend on the relative phase, and $^\otimes$ denotes which experimental data are not used to constrain parameters.

Observables	Exp. Data [1]	SU(3) IRA	Isospin Relations
$\mathcal{B}(\Sigma^+ \rightarrow p\pi^0)(\times 10^{-2})$	51.57 ± 0.30	$51.57 \pm 0.30^\ddagger$	$51.57 \pm 0.30^\ddagger$
$\mathcal{B}(\Sigma^+ \rightarrow n\pi^+)(\times 10^{-2})$	48.31 ± 0.30	$48.31 \pm 0.30^\ddagger$	$48.31 \pm 0.30^\ddagger$
$\mathcal{B}(\Sigma^- \rightarrow n\pi^-)(\times 10^{-2})$	99.848 ± 0.005	$99.848 \pm 0.005^\ddagger$	$99.848 \pm 0.005^\ddagger$
$\mathcal{B}(\Sigma^0 \rightarrow p\pi^-)(\times 10^{-10})$	\dots	4.82 ± 0.49	4.82 ± 0.50
$\mathcal{B}(\Sigma^0 \rightarrow n\pi^0)(\times 10^{-10})$	\dots	\dots	2.41 ± 0.27
$\mathcal{B}(\Lambda^0 \rightarrow p\pi^-)(\times 10^{-2})$	63.9 ± 0.5	$64.19 \pm 0.21^\ddagger$	\dots
$\mathcal{B}(\Lambda^0 \rightarrow n\pi^0)(\times 10^{-2})$	35.8 ± 0.5	$35.42 \pm 0.12^\ddagger$	\dots
$\mathcal{B}(\Xi^- \rightarrow \Lambda^0\pi^-)(\times 10^{-2})$	99.887 ± 0.035	$99.887 \pm 0.035^\ddagger$	\dots
$\mathcal{B}(\Xi^0 \rightarrow \Lambda^0\pi^0)(\times 10^{-2})$	99.524 ± 0.012	$80.016 \pm 3.746^\otimes$	\dots

$$\begin{aligned}
A(\Sigma^- \rightarrow n\pi^-) &= -\frac{\sqrt{2}}{3} \left(A_{\frac{1}{2}} - A_{\frac{3}{2}} \right), \\
A(\Sigma^0 \rightarrow p\pi^-) &= A_{\frac{3}{2}}, \\
A(\Sigma^0 \rightarrow n\pi^0) &= \frac{1}{3} \left(A_{\frac{1}{2}} + 2A_{\frac{3}{2}} \right).
\end{aligned} \tag{37}$$

There are three real parameters ($A_{\frac{1}{2}}, A_{\frac{3}{2}} e^{i\phi_{13}}$) in Eq. (37). Using the data of $\mathcal{B}(\Sigma^+ \rightarrow p\pi^0, \Sigma^+ \rightarrow n\pi^+, \Sigma^- \rightarrow n\pi^-)$, one can get $\mathcal{B}(\Sigma^0 \rightarrow p\pi^-)$ and $\mathcal{B}(\Sigma^0 \rightarrow n\pi^0)$, which are listed in the last column of Tab. VII. We can see that SU(3) IRA and isospin relations give the consistent predictions for $\mathcal{B}(\Sigma^0 \rightarrow p\pi^-)$.

For $\Lambda^0 \rightarrow p\pi^-, n\pi^0$ decays, there is only one parameter A_4 . We first get the value of $|A_4|$ from the data of $\mathcal{B}(\Lambda^0 \rightarrow p\pi^-)$, then further considering the experimental data of $\mathcal{B}(\Lambda^0 \rightarrow n\pi^0)$, finally give the predictions of $\mathcal{B}(\Lambda^0 \rightarrow p\pi^-, n\pi^0)$ in the third column of Tab. VII. One can see that the data of both $\mathcal{B}(\Lambda^0 \rightarrow p\pi^-)$ and $\mathcal{B}(\Lambda^0 \rightarrow n\pi^0)$ give the effective bounds on the parameter $|A_4|$, and the IRA predictions for $\mathcal{B}(\Lambda^0 \rightarrow p\pi^-, n\pi^0)$ are in agreement with the present data. Noted that, if only considering the experimental constraint from $\mathcal{B}(\Lambda^0 \rightarrow p\pi^-)$, the prediction of $\mathcal{B}(\Lambda^0 \rightarrow p\pi^-)$ given in the third column of Tab. VII, would be completely the same as the experimental datum. The slight difference between the prediction and datum comes from the experimental constraint of $\mathcal{B}(\Lambda^0 \rightarrow n\pi^0)$.

For $\Xi^- \rightarrow \Lambda^0\pi^-$ and $\Xi^0 \rightarrow \Lambda^0\pi^0$ decays, there is only one parameter A_5 . We use the data of $\mathcal{B}(\Xi^- \rightarrow \Lambda^0\pi^-)$ to obtain $|A_5|$, and then predict $\mathcal{B}(\Xi^0 \rightarrow \Lambda^0\pi^0)$. We obtain $\mathcal{B}(\Xi^0 \rightarrow \Lambda^0\pi^0) = (80.016 \pm 3.746)\%$, which is about 16% smaller than its data. The reason could be that the neglected C_+ term or SU(3) breaking effects might give a contribution of a few percent level to $\mathcal{B}(\Xi^- \rightarrow \Lambda^0\pi^-)$ and $\mathcal{B}(\Xi^0 \rightarrow \Lambda^0\pi^0)$.

2. $T_{10} \rightarrow T_8 M_8$ weak decays

Feynman diagrams for $T_{10} \rightarrow T_8 M_8$ nonleptonic decays are also displayed in Fig. 3, and the SU(3) IRA amplitudes are

$$\begin{aligned}
 A(T_{10} \rightarrow T_8 M_8)^{IRA} = & \bar{a}_1 H(4)_m^{lk}(T_{10})^{nij}(T_8)_{[ik]j}(M_8)_l^m + \bar{a}_2 H(4)_m^{lk}(T_{10})^{nij}(T_8)_{[jk]i}(M_8)_l^m \\
 & + \bar{b}_1 H(4)_m^{lk}(T_{10})^{nij}(T_8)_{[kl]i}(M_8)_j^m + \bar{b}_2 H(4)_m^{lk}(T_{10})^{nij}(T_8)_{[ki]l}(M_8)_j^m + \bar{b}_3 H(4)_m^{lk}(T_{10})^{nij}(T_8)_{[il]k}(M_8)_j^m \\
 & + \bar{c}_1 H(4)_j^{lk}(T_{10})^{nij}(T_8)_{[km]i}(M_8)_l^m + \bar{c}_2 H(4)_j^{lk}(T_{10})^{nij}(T_8)_{[ki]m}(M_8)_l^m + \bar{c}_3 H(4)_j^{lk}(T_{10})^{nij}(T_8)_{[im]k}(M_8)_j^m \\
 & + \bar{d}_1 H(4)_j^{lk}(T_{10})^{nij}(T_8)_{[mk]l}(M_8)_i^m + \bar{d}_2 H(4)_j^{lk}(T_{10})^{nij}(T_8)_{[ml]k}(M_8)_i^m + \bar{d}_3 H(4)_j^{lk}(T_{10})^{nij}(T_8)_{[kl]m}(M_8)_i^m \\
 & + \bar{e}_1 H(\bar{2})^k(T_{10})^{nij}(T_8)_{[im]j}(M_8)_k^m + \bar{e}_2 H(\bar{2})^k(T_{10})^{nij}(T_8)_{[jm]i}(M_8)_k^m \\
 & + \bar{f}_1 H(\bar{2})^k(T_{10})^{nij}(T_8)_{[ki]m}(M_8)_j^m + \bar{f}_2 H(\bar{2})^k(T_{10})^{nij}(T_8)_{[km]i}(M_8)_j^m + \bar{f}_3 H(\bar{2})^k(T_{10})^{nij}(T_8)_{[im]k}(M_8)_j^m.
 \end{aligned} \tag{38}$$

Considering $H(4)_m^{lk}$ and $(T_{10})^{nij}$ is symmetric in upper indices, we have the relations

$$\bar{a}_2 = \bar{a}_1, \quad \bar{b}_1 = 0, \quad \bar{b}_3 = -\bar{b}_2, \quad \bar{d}_2 = \bar{d}_1, \quad \bar{d}_3 = 0, \quad \bar{e}_2 = \bar{e}_1. \tag{39}$$

Then Eq. (38) can be simplified as

$$\begin{aligned}
 A(T_{10} \rightarrow T_8 M_8)^{IRA,J} = & \bar{a}_1 H(4)_m^{lk}(T_{10})^{nij}(T_8)_{[ik]j}(M_8)_l^m + \bar{b}_2 H(4)_m^{lk}(T_{10})^{nij}(T_8)_{[ki]l}(M_8)_j^m \\
 & + \bar{c}_1 H(4)_j^{lk}(T_{10})^{nij}(T_8)_{[km]i}(M_8)_l^m + \bar{c}_2 H(4)_j^{lk}(T_{10})^{nij}(T_8)_{[ki]m}(M_8)_l^m + \bar{c}_3 H(4)_j^{lk}(T_{10})^{nij}(T_8)_{[im]k}(M_8)_j^m \\
 & + \bar{d}_1 H(4)_j^{lk}(T_{10})^{nij}(T_8)_{[mk]l}(M_8)_i^m + \bar{e}_1 H(\bar{2})^k(T_{10})^{nij}(T_8)_{[im]j}(M_8)_k^m \\
 & + \bar{f}_1 H(\bar{2})^k(T_{10})^{nij}(T_8)_{[ki]m}(M_8)_j^m + \bar{f}_2 H(\bar{2})^k(T_{10})^{nij}(T_8)_{[km]i}(M_8)_j^m + \bar{f}_3 H(\bar{2})^k(T_{10})^{nij}(T_8)_{[im]k}(M_8)_j^m.
 \end{aligned} \tag{40}$$

The IRA amplitudes for $T_{10} \rightarrow T_8 P_8$ weak decays are listed in Tab. VIII, and the IRA amplitudes for $T_{10} \rightarrow T_8 V_8$ weak decays have similar relations. If neglecting $H(\bar{4})_2^{22}$ terms and c_i terms in $H(4)_1^{12}$, and redefining the parameters

$$\begin{aligned}
 \bar{A}_1 &= 2(\bar{a}_1 + \bar{e}_1), \\
 \bar{A}_2 &= 2(-\bar{a}_1 + \bar{e}_1), \\
 \bar{A}_3 &= 2(\bar{f}_1 + 2\bar{f}_2 + \bar{f}_3),
 \end{aligned} \tag{41}$$

the six decay amplitudes can be given in simpler forms, which are shown in the last column of Tab. VIII. Furthermore, we have the relation $A(\Xi^{*-} \rightarrow \Sigma^0 \pi^-) = A(\Xi^{*-} \rightarrow \Sigma^- \pi^0)$ if only considering the dominant $H(\bar{2})^2$ contributions.

The branching ratios of $T_{10} \rightarrow T_8 P_8$ can be obtained in terms of IRA amplitudes

$$\mathcal{B}(T_{10A} \rightarrow T_{8B} P_8) = \frac{\tau_A |p_{cm}|}{16\pi m_A^2} |A(T_{10A} \rightarrow T_{8B} P_8)|^2, \tag{42}$$

and the mass difference in $A(T_{10A} \rightarrow T_{8B} P_8)$, which is similar to Eq. (35), is also considered.

At present, only three Ω^- decay modes have been measured

$$\begin{aligned}
 \mathcal{B}(\Omega^- \rightarrow \Xi^0 \pi^-)(\times 10^{-2}) &= (23.6 \pm 0.7) \times 10^{-2}, \\
 \mathcal{B}(\Omega^- \rightarrow \Xi^- \pi^0)(\times 10^{-2}) &= (8.6 \pm 0.4) \times 10^{-2}, \\
 \mathcal{B}(\Omega^- \rightarrow \Lambda^0 K^-)(\times 10^{-2}) &= (67.8 \pm 0.7) \times 10^{-2}.
 \end{aligned} \tag{43}$$

TABLE VIII: The SU(3) IRA amplitudes of $T_{10} \rightarrow T_8 M_8$ weak decays.

Amplitudes	$H(4)_1^{12} = \frac{1}{3}$	$H(4)_2^{22} = -\frac{1}{3}$	$H(\bar{2})^2 = 1$	Simplified Amplitudes
$A(\Omega^- \rightarrow \Xi^0 \pi^-)$	$2\bar{a}_1$		$2\bar{e}_1$	\bar{A}_1
$\sqrt{2}A(\Omega^- \rightarrow \Xi^- \pi^0)$	$-2\bar{a}_1$	$2\bar{a}_1$	$2\bar{e}_1$	\bar{A}_2
$\sqrt{6}A(\Omega^- \rightarrow \Lambda^0 K^-)$			$\bar{f}_1 + 2\bar{f}_2 + \bar{f}_3$	\bar{A}_3
$3\sqrt{2}A(\Xi^{*-} \rightarrow \Lambda^0 \pi^-)$	$6\bar{a}_1$	$2\bar{c}_1 + \bar{c}_2 + \bar{c}_3$	$6\bar{e}_1 + \bar{f}_1 + 2\bar{f}_2 + \bar{f}_3$	$3\bar{A}_1 + \bar{A}_3$
$\sqrt{6}A(\Xi^{*-} \rightarrow \Sigma^0 \pi^-)$	$2\bar{a}_1 - 4\bar{b}_2$	$\bar{c}_3 - \bar{c}_2$	$2\bar{e}_1 - \bar{f}_1 + \bar{f}_3$	
$\sqrt{6}A(\Xi^{*-} \rightarrow \Sigma^- \pi^0)$	$-2\bar{a}_1$	$2\bar{a}_1 - 2\bar{b}_2 + \bar{c}_3 - \bar{c}_2$	$2\bar{e}_1 - \bar{f}_1 + \bar{f}_3$	
$\sqrt{3}A(\Xi^{*0} \rightarrow \Sigma^+ \pi^-)$	$2\bar{a}_1 + \bar{c}_3 - \bar{c}_2$		$2\bar{e}_1$	\bar{A}_1
$\sqrt{3}A(\Xi^{*0} \rightarrow \Sigma^- \pi^+)$	$\bar{c}_2 - \bar{c}_3$	$2\bar{b}_2$	$\bar{f}_1 - \bar{f}_3$	
$6A(\Xi^{*0} \rightarrow \Lambda^0 \pi^0)$	$-6\bar{a}_1 + 2(2\bar{c}_1 + \bar{c}_2 + \bar{c}_3)$	$6\bar{a}_1$	$6\bar{e}_1 + \bar{f}_1 + 2\bar{f}_2 + \bar{f}_3$	$3\bar{A}_2 + \bar{A}_3$
$2\sqrt{3}A(\Xi^{*0} \rightarrow \Sigma^0 \pi^0)$	$2\bar{a}_1 - 4\bar{b}_2$	$-2\bar{a}_1$	$-2\bar{e}_1 - \bar{f}_1 + \bar{f}_3$	
$\sqrt{3}A(\Xi^{*-} \rightarrow n K^-)$	$2\bar{b}_2$	$2\bar{d}_1$	$-\bar{f}_2 - \bar{f}_3$	
$\sqrt{3}A(\Sigma^{*-} \rightarrow n \pi^-)$	$-2\bar{a}_1 + 2\bar{b}_2$	$-\bar{c}_1 - \bar{c}_3 + 2\bar{d}_1$	$-2\bar{e}_1 - \bar{f}_2 - \bar{f}_3$	

We obtain that $|\bar{A}_1| = 8.54 \pm 0.19$, $|\bar{A}_2| = 7.47 \pm 0.23$ and $|\bar{A}_3| = 5.36 \pm 0.08$ from the data of $\mathcal{B}(\Omega^- \rightarrow \Xi^0 \pi^-)$, $\mathcal{B}(\Omega^- \rightarrow \Xi^- \pi^0)$ and $\mathcal{B}(\Omega^- \rightarrow \Lambda^0 K^-)$, respectively. Then we predict that

$$\begin{aligned}
\mathcal{B}(\Xi^{*-} \rightarrow \Lambda^0 \pi^-) &= (1.06 \pm 0.90) \times 10^{-12}, \\
\mathcal{B}(\Xi^{*0} \rightarrow \Sigma^+ \pi^-) &= (5.96 \pm 0.58) \times 10^{-14}, \\
\mathcal{B}(\Xi^{*0} \rightarrow \Lambda^0 \pi^0) &= (5.02 \pm 4.06) \times 10^{-13},
\end{aligned} \tag{44}$$

where the prediction of $\mathcal{B}(\Xi^{*-} \rightarrow \Lambda^0 \pi^-)$ depends on the relative phase between \bar{A}_1 and \bar{A}_3 , and the prediction of $\mathcal{B}(\Xi^{*0} \rightarrow \Lambda^0 \pi^0)$ depends on the relative phase between \bar{A}_2 and \bar{A}_3 .

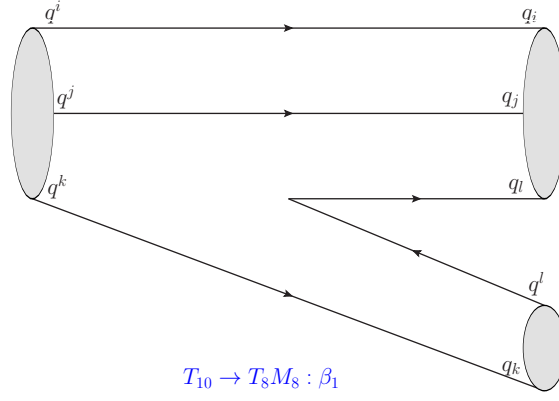
B. Electromagnetic or strong decays of light baryons

The light baryons T_{10} can also decay through electromagnetic or strong interactions. The Feynman diagram of electromagnetic or strong (ES) decays of T_{10} is shown in Fig. 4. In this case, we only need consider the SU(3) symmetry between initial and final states. The SU(3) IRA amplitude of $T_{10} \rightarrow T_8 M_8$ ES decay is

$$A(T_{10} \rightarrow T_8 M_8)^{ES,IRA} = \beta_1 (T_{10})^{ijk} (T_8)_{[il]j} (M_8)_k^l. \tag{45}$$

There is only one parameter β_1 for these IRA amplitude. The IRA amplitudes of all the ES $T_{10} \rightarrow T_8 P_8$ decays are given in Tab. IX.

For these ES decays, only three branching ratios are measured, which are given in Tab. X. We first get $|\beta_1|$ from the data of $\mathcal{B}(\Sigma^* \rightarrow \Sigma \pi)$, then also consider the experimental constraint from $\mathcal{B}(\Sigma^* \rightarrow \Lambda \pi)$, and finally give the

FIG. 4: Feynman diagram of IRA for $T_{10} \rightarrow T_8 M_8$ ES decays.TABLE IX: The IRA amplitudes of $T_{10} \rightarrow T_8 P_8$ ES decays under the SU(3) flavor symmetry.

Amplitudes	SU(3) IRA amplitudes
$\sqrt{6}A(\Sigma^{*+} \rightarrow \Sigma^0 \pi^+)$	β_1
$\sqrt{6}A(\Sigma^{*+} \rightarrow \Sigma^+ \pi^0)$	β_1
$2\sqrt{6}A(\Sigma^{*0} \rightarrow \Sigma^0 \pi^0)$	0
$\sqrt{6}A(\Sigma^{*0} \rightarrow \Sigma^+ \pi^-)$	β_1
$\sqrt{6}A(\Sigma^{*0} \rightarrow \Sigma^- \pi^+)$	$-\beta_1$
$\sqrt{6}A(\Sigma^{*-} \rightarrow \Sigma^- \pi^0)$	β_1
$\sqrt{6}A(\Sigma^{*-} \rightarrow \Sigma^0 \pi^-)$	β_1
$3\sqrt{2}A(\Sigma^{*+} \rightarrow \Lambda^0 \pi^+)$	$-3\beta_1$
$6\sqrt{2}A(\Sigma^{*0} \rightarrow \Lambda^0 \pi^0)$	$6\beta_1$
$3\sqrt{2}A(\Sigma^{*-} \rightarrow \Lambda^0 \pi^-)$	$3\beta_1$
$\sqrt{6}A(\Xi^{*0} \rightarrow \Xi^0 \pi^0)$	β_1
$\sqrt{3}A(\Xi^{*0} \rightarrow \Xi^- \pi^+)$	$-\beta_1$
$\sqrt{6}A(\Xi^{*-} \rightarrow \Xi^- \pi^0)$	β_1
$\sqrt{3}A(\Xi^{*-} \rightarrow \Xi^0 \pi^-)$	β_1

predictions of other specific branching ratios. Our SU(3) IRA predictions are given in Tab. X, where one can see that, within 1σ error, the experimental result of $\mathcal{B}(\Sigma^* \rightarrow \Lambda\pi)$ can effectively constrain $|\beta_1|$. In addition, when IRA predictions are consistent with the data of $\mathcal{B}(\Sigma^* \rightarrow \Sigma\pi)$ and $\mathcal{B}(\Sigma^* \rightarrow \Lambda\pi)$, the prediction of $\mathcal{B}(\Xi^* \rightarrow \Xi\pi)$ is slightly larger than its experimental result, which might imply that the SU(3) breaking effects could give visible contributions to $\mathcal{B}(\Xi^* \rightarrow \Xi\pi)$. Nevertheless, the prediction and experimental data of $\mathcal{B}(\Xi^* \rightarrow \Xi\pi)$ can be consistent within 1.3σ error. And moreover, the decay width predictions of $\Xi^{*0} \rightarrow \Xi\pi$ and $\Xi^{*-} \rightarrow \Xi\pi$ in the chiral quark-soliton model are

TABLE X: Branching ratios of $T_{10} \rightarrow T_8 P_8$ ES decays within 1σ error. † denotes which experimental data have been used to give the effective constraints on the parameters, and $^\otimes$ denotes which experimental data are not used to constrain parameters.

Branching ratios	Exp.	SU(3) IRA
$\mathcal{B}(\Sigma^{*+} \rightarrow \Sigma^0 \pi^+)(\times 10^{-2})$...	5.34 ± 0.50
$\mathcal{B}(\Sigma^{*+} \rightarrow \Sigma^+ \pi^0)(\times 10^{-2})$...	6.59 ± 0.61
$\mathcal{B}(\Sigma^{*0} \rightarrow \Sigma^0 \pi^0)(\times 10^{-2})$...	0
$\mathcal{B}(\Sigma^{*0} \rightarrow \Sigma^+ \pi^-)(\times 10^{-2})$...	6.20 ± 0.78
$\mathcal{B}(\Sigma^{*0} \rightarrow \Sigma^- \pi^+)(\times 10^{-2})$...	4.71 ± 0.59
$\mathcal{B}(\Sigma^{*-} \rightarrow \Sigma^- \pi^0)(\times 10^{-2})$...	5.40 ± 0.60
$\mathcal{B}(\Sigma^{*-} \rightarrow \Sigma^0 \pi^-)(\times 10^{-2})$...	5.66 ± 0.63
$\mathcal{B}(\Sigma^* \rightarrow \Sigma \pi)(\times 10^{-2})$	11.7 ± 1.5	11.24 ± 0.28
$\mathcal{B}(\Sigma^{*+} \rightarrow \Lambda^0 \pi^+)(\times 10^{-2})$...	86.14 ± 7.62
$\mathcal{B}(\Sigma^{*0} \rightarrow \Lambda^0 \pi^0)(\times 10^{-2})$...	91.68 ± 11.36
$\mathcal{B}(\Sigma^{*-} \rightarrow \Lambda^0 \pi^-)(\times 10^{-2})$...	84.44 ± 8.96
$\mathcal{B}(\Sigma^* \rightarrow \Lambda^0 \pi)(\times 10^{-2})$	87.0 ± 1.5	$87.00 \pm 1.50^\dagger$
$\mathcal{B}(\Xi^{*0} \rightarrow \Xi^0 \pi^0)(\times 10^{-2})$...	48.22 ± 6.55
$\mathcal{B}(\Xi^{*0} \rightarrow \Xi^- \pi^+)(\times 10^{-2})$...	76.23 ± 10.32
$\mathcal{B}(\Xi^{*-} \rightarrow \Xi^- \pi^0)(\times 10^{-2})$...	43.05 ± 11.01
$\mathcal{B}(\Xi^{*-} \rightarrow \Xi^0 \pi^-)(\times 10^{-2})$...	94.33 ± 24.12
$\mathcal{B}(\Xi^* \rightarrow \Xi \pi)(\times 10^{-2})$	100	$131.01 \pm 24.40^\otimes$

also slightly larger than their experimental data [62].

Note that the ES $T_8 \rightarrow T_8 P_8$ decays and the ES $T_{10} \rightarrow T_8 K$ decays are not allowed by the phase space, since the sum of final hadron masses is larger than the mass of initial state.

IV. SUMMARY

Light baryon decays play very important role in testing the SM and searching for new physics beyond the SM. Many decay modes have been measured and some decays can be studied at BESIII and LHCb experiments now. Motivated by this, we have analyzed the semileptonic decays and two-body nonleptonic decays of light baryon octet and decuplet by using the irreducible representation approach to test the SU(3) flavor symmetry. Our main results can be summarized as follows:

- **Semileptonic light baryon decays:** We find that all branching ratio predictions of octet and decuplet baryons through $s \rightarrow u \ell^- \bar{\nu}_\ell$ and $d \rightarrow u e^- \bar{\nu}_e$ transitions with SU(3) IRA in S_2 case are quite consistent with present

experimental measurements within 1σ error. We predict that $\mathcal{B}(\Xi^- \rightarrow \Sigma^0 \mu^- \bar{\nu}_\mu)$ and $\mathcal{B}(\Omega^- \rightarrow \Xi^0 \mu^- \bar{\nu}_\mu)$ are at the order of magnitudes of 10^{-6} and 10^{-3} , respectively, and $\mathcal{B}(\Sigma^- \rightarrow \Sigma^0 e^- \bar{\nu}_e, \Xi^- \rightarrow \Xi^0 e^- \bar{\nu}_e)$ are at the order of 10^{-10} . These decays are promising to be observed by the BESIII and LHCb experiments or the future experiments. However, other branching ratios, which are in the range of $10^{-20} - 10^{-13}$, may not be measured for a long time. Moreover, the longitudinal branching ratios of decays of $T_{8A} \rightarrow T_{8B} \ell^- \bar{\nu}_\ell$ are also predicted in this work.

- **Nonleptonic two-body light baryon decays:** We obtain the relations of different decay amplitudes by the SU(3) IRA and isospin symmetry. In $T_8 \rightarrow T_8 P_8$ weak decays, we find that SU(3) IRA predictions of the branching ratios of Σ, Λ baryons are consistent with present experimental data, $\mathcal{B}(\Sigma^0 \rightarrow p \pi^-, n \pi^0)$ are at the order of 10^{-10} by the SU(3) IRA or isospin symmetry, and the neglected C_+ terms or SU(3) symmetry breaking effects might give a contribution of a few percent to the two branching ratios of $\Xi \rightarrow \Lambda \pi$. In $T_{10} \rightarrow T_8 P$ weak decays, we predict that $\mathcal{B}(\Xi^{*-} \rightarrow \Lambda^0 \pi^-)$, $\mathcal{B}(\Xi^{*0} \rightarrow \Lambda^0 \pi^0)$ and $\mathcal{B}(\Xi^{*0} \rightarrow \Sigma^+ \pi^-)$ are at the orders of 10^{-12} , 10^{-13} and 10^{-14} , respectively. In $T_{10} \rightarrow T_8 P_8$ ES decays, when IRA predictions are consistent with the data of $\mathcal{B}(\Sigma^* \rightarrow \Sigma \pi)$ and $\mathcal{B}(\Sigma^* \rightarrow \Lambda \pi)$, the prediction of $\mathcal{B}(\Xi^* \rightarrow \Xi \pi)$ is slightly larger than experimental data, which imply that the SU(3) symmetry breaking effects could give visible contributions to $\mathcal{B}(\Xi^* \rightarrow \Xi \pi)$. In addition, we given all the specific branching ratio predictions for these $T_{10} \rightarrow T_8 P_8$ ES decays.

Although flavor SU(3) symmetry is approximate, it can still provide us very useful information about these decays. According to our predictions, some branching ratios are accessible to the experiments at BESIII and LHCb. Our results in this work can be used to test SU(3) flavor symmetry approach in light baryon decays by the future experiments..

ACKNOWLEDGEMENTS

Ru-Min Wang thanks Wei Wang for helpful communications. The work was supported by the National Natural Science Foundation of China (Contract Nos. 11675137, 11875168 and 11875054), the Joint Large-Scale Scientific Facility Funds of the NSFC and CAS under Contract No. U1532257, CAS under Contract No. QYZDJ-SSWSLH003; and and the National Key Basic Research Program of China under Contract No. 2015CB856700.

References

-
- [1] M. Tanabashi et al. (Particle Data Group), Phys. Rev. D **98**, 030001 (2018).
 - [2] H. B. Li, Front. Phys. (Beijing) **12**, no. 5, 121301 (2017) [arXiv:1612.01775 [hep-ex]].
 - [3] I. I. Bigi, X. W. Kang and H. B. Li, Chin. Phys. C **42**, no. 1, 013101 (2018)
 - [4] D. M. Asner *et al.*, Int. J. Mod. Phys. A **24**, S1 (2009) [arXiv:0809.1869 [hep-ex]].
 - [5] M. Ablikim *et al.* (BESIII Collaboration), Nature Physics (2019), <https://doi.org/10.1038/s41567-019-0494-8>.
 - [6] R. Aaij *et al.* (LHCb Collaboration), Phys. Rev. Lett. **120**, no. 22, 221803 (2018) [arXiv:1712.08606 [hep-ex]].
 - [7] A. A. Alves Junior *et al.*, JHEP **1905**, 048 (2019), [arXiv:1808.03477 [hep-ex]].

- [8] S. Weinberg, J. Phys. Conf. Ser. **196**, 012002 (2009).
- [9] N. Severijns, M. Beck and O. Naviliat-Cuncic, Rev. Mod. Phys. **78**, 991 (2006) [nucl-ex/0605029].
- [10] N. Cabibbo, Phys. Rev. Lett. **10**, 531 (1963).
- [11] V. Cirigliano, M. Gonzalez-Alonso and M. L. Graesser, JHEP **1302**, 046 (2013) [arXiv:1210.4553 [hep-ph]].
- [12] H. M. Chang, M. Gonzalez-Alonso and J. Martin Camalich, Phys. Rev. Lett. **114**, no. 16, 161802 (2015) [arXiv:1412.8484 [hep-ph]].
- [13] X. G. He, Eur. Phys. J. C **9**, 443 (1999) [hep-ph/9810397].
- [14] X. G. He, Y. K. Hsiao, J. Q. Shi, Y. L. Wu and Y. F. Zhou, Phys. Rev. D **64**, 034002 (2001) [hep-ph/0011337].
- [15] H. K. Fu, X. G. He and Y. K. Hsiao, Phys. Rev. D **69**, 074002 (2004) [hep-ph/0304242].
- [16] Y. K. Hsiao, C. F. Chang and X. G. He, Phys. Rev. D **93**, no. 11, 114002 (2016) [arXiv:1512.09223 [hep-ph]].
- [17] X. G. He and G. N. Li, Phys. Lett. B **750**, 82 (2015) [arXiv:1501.00646 [hep-ph]].
- [18] M. Gronau, O. F. Hernandez, D. London and J. L. Rosner, Phys. Rev. D **50**, 4529 (1994) [hep-ph/9404283].
- [19] M. Gronau, O. F. Hernandez, D. London and J. L. Rosner, Phys. Rev. D **52**, 6356 (1995) [hep-ph/9504326].
- [20] S. H. Zhou, Q. A. Zhang, W. R. Lyu and C. D. L, Eur. Phys. J. C **77**, no. 2, 125 (2017) [arXiv:1608.02819 [hep-ph]].
- [21] H. Y. Cheng, C. W. Chiang and A. L. Kuo, Phys. Rev. D **91**, no. 1, 014011 (2015) [arXiv:1409.5026 [hep-ph]].
- [22] M. He, X. G. He and G. N. Li, Phys. Rev. D **92**, no. 3, 036010 (2015) [arXiv:1507.07990 [hep-ph]].
- [23] N. G. Deshpande and X. G. He, Phys. Rev. Lett. **75**, 1703 (1995) [hep-ph/9412393].
- [24] S. Shivashankara, W. Wu and A. Datta, Phys. Rev. D **91**, 115003 (2015) [arXiv:1502.07230 [hep-ph]].
- [25] Y. Grossman and D. J. Robinson, JHEP **1304**, 067 (2013) [arXiv:1211.3361 [hep-ph]].
- [26] D. Pirtskhalava and P. Uttayarat, Phys. Lett. B **712**, 81 (2012) [arXiv:1112.5451 [hep-ph]].
- [27] H. Y. Cheng and C. W. Chiang, Phys. Rev. D **86**, 014014 (2012) [arXiv:1205.0580 [hep-ph]].
- [28] M. J. Savage and R. P. Springer, Phys. Rev. D **42**, 1527 (1990).
- [29] M. J. Savage, Phys. Lett. B **257**, 414 (1991).
- [30] G. Altarelli, N. Cabibbo and L. Maiani, Phys. Lett. **57B**, 277 (1975).
- [31] C. D. L, W. Wang and F. S. Yu, Phys. Rev. D **93**, no. 5, 056008 (2016) [arXiv:1601.04241 [hep-ph]].
- [32] C. Q. Geng, Y. K. Hsiao, Y. H. Lin and L. L. Liu, Phys. Lett. B **776**, 265 (2018) [arXiv:1708.02460 [hep-ph]].
- [33] C. Q. Geng, Y. K. Hsiao, C. W. Liu and T. H. Tsai, Phys. Rev. D **97**, no. 7, 073006 (2018) [arXiv:1801.03276 [hep-ph]].
- [34] C. Q. Geng, Y. K. Hsiao, C. W. Liu and T. H. Tsai, JHEP **1711**, 147 (2017) [arXiv:1709.00808 [hep-ph]].
- [35] C. Q. Geng, C. W. Liu, T. H. Tsai and S. W. Yeh, arXiv:1901.05610 [hep-ph].
- [36] W. Wang, Z. P. Xing and J. Xu, Eur. Phys. J. C **77**, no. 11, 800 (2017) [arXiv:1707.06570 [hep-ph]].
- [37] D. Wang, arXiv:1901.01776 [hep-ph].
- [38] D. Wang, P. F. Guo, W. H. Long and F. S. Yu, JHEP **1803**, 066 (2018) [arXiv:1709.09873 [hep-ph]].
- [39] S. Müller, U. Nierste and S. Schacht, Phys. Rev. D **92**, no. 1, 014004 (2015) [arXiv:1503.06759 [hep-ph]].
- [40] J. M. Gaillard and G. Sauvage, Ann. Rev. Nucl. Part. Sci. **34**, 351 (1984).
- [41] T. N. Pham, Phys. Rev. D **87**, no. 1, 016002 (2013) [arXiv:1210.3981 [hep-ph]].
- [42] M. E. Carrillo-Serrano, I. C. Cloet and A. W. Thomas, Phys. Rev. C **90**, no. 6, 064316 (2014) [arXiv:1409.1653 [nucl-th]].
- [43] R. Flores-Mendieta, E. E. Jenkins and A. V. Manohar, Phys. Rev. D **58**, 094028 (1998) [hep-ph/9805416].
- [44] A. Kadeer, J. G. Korner and U. Moosbrugger, Eur. Phys. J. C **59**, 27 (2009) [hep-ph/0511019].
- [45] S. Sasaki, Phys. Rev. D **86**, 114502 (2012) [arXiv:1209.6115 [hep-lat]].
- [46] S. Sasaki and T. Yamazaki, Phys. Rev. D **79**, 074508 (2009) [arXiv:0811.1406 [hep-ph]].
- [47] G. Villadoro, Phys. Rev. D **74**, 014018 (2006) [hep-ph/0603226].
- [48] A. Lacour, B. Kubis and U. G. Meissner, JHEP **0710**, 083 (2007) [arXiv:0708.3957 [hep-ph]].
- [49] A. Faessler, T. Gutsche, B. R. Holstein, M. A. Ivanov, J. G. Korner and V. E. Lyubovitskij, Phys. Rev. D **78**, 094005 (2008) [arXiv:0809.4159 [hep-ph]].
- [50] D. Guadagnoli, V. Lubicz, M. Papinutto and S. Simula, Nucl. Phys. B **761**, 63 (2007) [hep-ph/0606181].

- [51] N. Cabibbo, E. C. Swallow and R. Winston, *Ann. Rev. Nucl. Part. Sci.* **53**, 39 (2003) [hep-ph/0307298].
- [52] T. Ledwig, A. Silva, H. C. Kim and K. Goeke, *JHEP* **0807**, 132 (2008) [arXiv:0806.4072 [hep-ph]].
- [53] A. Faessler, T. Gutsche, B. R. Holstein and V. E. Lyubovitskij, *Phys. Rev. D* **77**, 114007 (2008) [arXiv:0712.3437 [hep-ph]].
- [54] G. S. Yang and H. C. Kim, *Phys. Rev. C* **92**, 035206 (2015) [arXiv:1504.04453 [hep-ph]].
- [55] G. Buchalla, A. J. Buras and M. E. Lautenbacher, *Rev. Mod. Phys.* **68**, 1125 (1996) [hep-ph/9512380].
- [56] E. E. Jenkins, *Nucl. Phys. B* **375**, 561 (1992).
- [57] A. Abd El-Hady and J. Tandean, *Phys. Rev. D* **61**, 114014 (2000) [hep-ph/9908498].
- [58] R. Flores-Mendieta, *Phys. Rev. D* **99**, no. 9, 094033 (2019) [arXiv:1902.05602 [hep-ph]].
- [59] J. Tandean and G. Valencia, *Phys. Rev. D* **67**, 056001 (2003) [hep-ph/0211165].
- [60] B. Borasoy and E. Marco, *Phys. Rev. D* **67**, 114016 (2003) [hep-ph/0306175].
- [61] X. G. He, Y. J. Shi and W. Wang, arXiv:1811.03480 [hep-ph].
- [62] G. S. Yang and H. C. Kim, *Phys. Lett. B* **785**, 434 (2018) [arXiv:1807.09090 [hep-ph]].